Mathematics

http://www.aimspress.com/journal/Math

AIMS Mathematics, 11(6): 19177–19216.
DOI: 10.3934/math.2026781
Received: 23 February 2026
Revised: 06 May 2026
Accepted: 25 May 2026
Published: 30 June 2026

Research article

Data-driven complex network framework for risk dynamics and stability evaluations in renewable-integrated power systems

Tariq Ali[1,2,*], **Muzna Sarwar**[3,*], **Farrukh Jamal**[4], **Mohammad Hijji**[2], **Husam S. Samkari**[1,5], **Mohammed F. Allehyani**[5], **M. Ammad ud Din**[6] **and Muhammad Ayaz**[1,4]

[1] Artificial Intelligence and Sensing Technology Research Center (AIST), University of Tabuk, Tabuk 71491, Saudi Arabia
[2] Faculty of Computers and Information Technology, University of Tabuk, Tabuk, 71491, Saudi Arabia
[3] Department of Statistics, Faculty of Computing, Islamia University of Bahawalpur, Pakistan
[4] Department of Statistics, Faculty of Science, University of Tabuk, Tabuk, Saudi Arabia
[5] Department of Electrical Engineering, University of Tabuk, Tabuk, 47713, Saudi Arabia
[6] Lab-STICC, UMR 6285-CNRS, ENSTA, Institut Polytechnique de Paris, 29200 Brest, France

* **Correspondence:** Email: teshaq@ut.edu.sa, muznastatphd@gmail.com.

Abstract: The integration of renewable energy sources into modern power systems introduces stability and resilience challenges due to their intermittent and stochastic behavior. To address these issues, this study proposes an artificial intelligence (AI)-driven statistical complex network (AI-SCN) framework for stability assessments in renewable-integrated power grids. The framework models the grid as a weighted complex network, where the nodes represent generation, storage, and load units, and the edges capture electrical and statistical dependencies. By integrating network topology metrics with data-driven AI models, AI-SCN enables accurate stability margin estimation and resilience quantification under varying renewable penetration levels. Simulations on the Institute of Electrical and Electronics Engineers (IEEE) 39-bus and IEEE 118-bus systems show that AI-SCN outperforms conventional and long short-term memory (LSTM)-based approaches, achieving root mean square error (RMSE) values of 0.0185 and 0.0219, respectively, representing improvements of 40.7% and 58.9%. Furthermore, recovery time is reduced from 12.8 s to 8.4 s, demonstrating the system's enhanced recovery efficiency. These results confirm that AI-SCN offers a scalable and adaptive framework for improving stability and resilience in renewable-dominant power systems.

Keywords: complex network; power system stability; energy integration; resilience assessment; machine learning; computational complexity
Mathematics Subject Classification: 34A08, 68T07

1. Introduction

The global effort to deploy low-carbon energy systems has spurred rapid large-scale integration of renewable energy sources, solar photovoltaic, wind, biomass, and distributed storage technologies. While facilitating decarbonization of the energy supply and democratization of generation fleets, these developments place unprecedented structural and dynamic stressors on the power grids of today. Unlike conventional synchronous units, renewable units are intermittent, stochastic, and power-electronics based. They alter the system's inertia, damping, and stability limits [1–3]. Electricity networks become less coherent, and less dispatchable, and eventually transition to decentralized heterogeneous and nonlinearly coupled strongly dynamical systems with increasing renewable integration. Classical methods like eigenvalue analysis (small-signal stability) or deterministic contingency analysis were originally designed for grid systems that have high inertia and are predictable [4]. Linearized models and pre-selected contingencies may not account for renewables' variability and nonlinear effects [5]. They also tend to analyze components of the grid in isolation instead of coupled subsystems of the overall network.

Network science (also referred to as complex network theory) is used as an efficient methodology to study complex networks [6, 7]. Network science allows us to calculate a network's measures, such as degree centrality, clustering coefficient, betweeness centrality, network efficiency, etc., to identify influential nodes and bottlenecks in the power system's network topology [8, 9]. However, most of the existing literature relies only on the topological characteristics (static) of the power system without utilizing the available operational information. In contrast, artificial intelligence (AI)-based models such as deep neural networks, recurrent models, graph networks, etc., have demonstrated impressive performance for prediction and stability analysis tasks [10–12]. However, these models are often criticized for their lack of interpretability and for their lack of physical relevance to grid topology.

In order to address these issues, this paper presents an AI-driven statitical complex network (AI-SCN) for simplicity. The AI-SCN framework applies techniques from statistical dependency modeling, complex network topology characterization, and machine learning (ML) to enhance adaptability and provide a comprehensive platform for studying the stability and resilience of renewable-dominated energy systems. Specifically, in the AI-SCN framework, we model the power grid as a weighted, time-varying network whose nodes represent generators, renewable energy sources, storage devices, and loads, edges between nodes represent electrical coupling and statistically measured operational dependencies.

Unlike traditional static networks, AI-SCN includes a statistical correlation matrix and a sensitivity-based weighted matrix to form an integrated network topology. Moreover, the trained AI learns a nonlinear mapping of the space-time-coupled relationship between renewables' uncertainty and networks' condition to adjust the secure margin. In addition, network resilience is evaluated using a combined robustness index that considers efficiency, the ratio of the largest cluster, the cascade failure fraction, and the recovery fraction. To address the aforementioned challenges, this paper proposes a novel AI-SCN framework for assessing stability and resilience in renewable-integrated power systems. Unlike conventional approaches that treat the networks' topology and data-driven learning separately, the proposed method integrates physical electrical connectivity with statistical dependency modeling into a unified hybrid representation. As such, it facilitates topology-aware learning of both structural interactions and stochastic fluctuations due to renewable generation. Moreover, this framework unifies both stability prediction and resilience quantification. Together, these capabilities allow a comprehensive performance assessment of system's operation amid changing and uncertain conditions. Through simulations on standard test cases, we verify that the resulting method achieves enhanced prediction accuracy, robustness, and explainability relative to prior techniques. The main contributions of this work are summarized as follows.

- A novel AI-SCN framework is proposed that integrates a complex network topology with data-driven learning, enabling a unified representation of physical and statistical dependencies in power systems.
- A hybrid adjacency modeling approach is developed, combining electrical coupling and statistical correlations to capture both structural interactions and renewable-induced variability.
- A topology-aware spatiotemporal learning mechanism is introduced, leveraging graph-based feature extraction and temporal modeling to enhance the accuracy and interpretability of stability predictions.
- An integrated stability-resilience evaluation framework is formulated, incorporating multiple performance indicators, including stability margin, networks' robustness, and recovery characteristics.
- Extensive experimental validation on the Institute of Electrical and Electronics Engineers (IEEE) benchmark systems demonstrates that the proposed method outperforms conventional and state-of-the-art approaches in terms of accuracy, robustness, and computational efficiency.

The rest of the paper is structured as follows. Section 2 discusses the related work. Section 3 discusses the data and preprocessing framework. Section 4 shows the mathematical formulation of the AI-SCN topology and the statistical modeling process. Section 5 describes the detailed methodology of the proposed model. Section 6 details the experimental setup and benchmark renewable-integrated systems, discusses the simulations' results, and presents a comparative analysis. Section 7 concludes the paper and outlines future research directions.

2. Related work

The assessment of grid stability and robustness has been examined over the past years with the emergence of high penetration renewable energy sources, intermittency, distributed generation resources, and uncertainty in grid operations. Current mathematical models such as small-signal analysis or transient stability simulation, are unable to account for grid wide oscillations due to the incorporation of renewables and large-scale data [13]. Researchers have since proposed complex network theory-based frameworks, AI and ML models, and hybrid structural/data-driven methodologies.

2.1. Complex network perspectives

Complex network theory has been widely used to model power systems as graphs, enabling the structural analysis of connectivity, vulnerability, and the propagation of disturbances. A detailed review of definitions of resilience for the modern power system from the complex networks perspective, including both structural and operational resilience across preventive, inherent, and restorative strategies was presented by [14]. It was argued that topological analysis alone is insufficient to characterize a system's resilience under extreme events, motivating a movement toward holistic frameworks allowing for transitional states and operational data. Node centrality, clustering, and path length have been popular network metrics applied to quantifying a grid's robustness and evaluating important elements, but they tend to disregard statistical dependencies in operations.

2.2. *AI/ML for stability and control*

AI and ML techniques have become popular for addressing nonlinear dynamics, prediction, and adaptive control in power systems. The ML applications for different stability problems, such as voltage stability, transient stability, and small-signal stability were reviewed by Ćosić and Vokony [15]. The authors concluded that data-driven models may be capable of capturing such complex real-time dynamics. A comprehensive review of AI techniques for power systems' stability, control, and protection has been presented by Saxena et al. [16]. They also outlined the research challenges of integrating AI into smart grid operations. ML applications for analyzing the stability and contingency of smart grid. The authors noted that ML methods can improve decision-making but face limitations, such as data quality and the generalization of learning models, as discussed by Waheed and Li [17].

Beyond general AI applications, specialized reviews have examined the use of AI for resilience enhancement. A survey on ML applications in power system-related resilience analytics and operations, including outage prediction, stability assessment, emergency control, and restoration, was provided in Zaidi et al. [18]. There has been a recent increase in interest in data-driven approaches. A comprehensive survey about the applications of AI for improving microgrids' resilience from multiple perspectives, including the performance before, during, and after contingencies, was presented by Dineshkumar [19]. The paper also discussed some advanced AI techniques (such as deep learning) to enhance the resilience of a microgrid against both extreme events and daily grid disruptions with various applications, such as physical robustness and real-time grid control, etc. A survey on comprehensive AI techniques without specifically considering resilience (examples include AI for operational reliability, power system planning, and control), was provided by Zeriouh and Amara [20].

One of the most important challenges is to address the interpretability/embedding of physical intuition in AI models. AI models tend to be treated like a black box, where the prediction cannot be correlated with a relationship to the system's topology nor physical operation constraints. Trustworthy, secure deployment of AI within the grid infrastructure is also an active area of research [21].

2.3. *Hybrid and data-driven resilience studies*

Several studies have sought to integrate structural and data-driven methods. While complex networks studies capture static graph properties effectively, they often lack operational insights. Conversely, ML approaches are data-driven methods that often do not account for the networks' topology. The topology-data analytics frameworks mentioned above may assist in filling these gaps. For instance, cascading failures modeled using graph neural networks and deep learning inherently account for networks' topology allowing learning-based techniques to predict the cascading behavior of instabilities through the network. Joint topology operation behavior-resilience performance metric frameworks are not common, which presents an opportunity for AI-SCN.

Additionally, resilience metric studies need common definitions and quantifications of resilience to define how to measure the resilience of a system and its recovery processes. Resilience metrics for distribution systems have been extensively investigated, highlighting the fundamental differences between resilience and traditional reliability measures [22]. Research has also discussed fundamental resilience metrics. The existing literature suggests that resilience is a multifaceted concept that requires an integrated evaluation of a system's performance under both normal and disturbed operating conditions.

2.4. Critical summary and research gaps

In summary, the existing literature can be grouped into three main paradigms:

- **Topology/complex network approaches**: These provide structural insights but often lack dynamic operational data integration [23];
- **AI/ML models**: These capture nonlinear dynamics and predictive patterns but may ignore the networks' structure and physical interpretability [24–26];
- **Hybrid data-driven approaches**: Emerging methods combining topological and learning insights, though comprehensive resilience evaluation frameworks remain scarce.

The key gaps include the following:

- Limited integration of the structural topology with adaptive learning models for assessing resilience;
- Lack of standardized resilience metrics combining topology, dynamics, and recovery performance;
- Insufficient interpretability and deployment reliability in the AI models applied to power system analysis.

These gaps motivate the proposed AI-SCN framework, which unifies statistical complex networks modeling with AI-based dynamic learning to assess stability and resilience in renewable-integrated grids. Table 1 presents a comparison of representative related studies. In summary, the existing studies have explored topology-based analysis, AI-driven prediction, and hybrid modeling approaches for power systems' stability. However, these methods often address individual aspects in isolation. Recent advances in robust estimation, event-triggered control, and data-driven optimization for complex networked systems further highlight the importance of integrating learning, control, and topology in modern power systems [27–29]. The study in [30] focused on enhancing the composite anti-disturbance control framework by integrating efficient computational techniques and robust communication protocols, ensuring better performance in real-world networked systems with disturbances and actuator attacks, but did not address the computational complexity associated with the proposed control strategies in large-scale networked systems. Additionally, it assumed ideal communication channels, which may not be applicable in real-world scenarios with unreliable network conditions. These observations motivate the need for a unified framework that jointly captures structural, statistical, and dynamic characteristics, as proposed in this work.

Table 1. Comparative analysis of existing works with limitations.

Ref.	Domain	Method	Artificial intelligence	Network	Resilience	Limitation
[22]	Power distribution	Review	×	Grid	✓	Lacks quantitative validation
[23]	Transport	Network theory	×	Airline	✓	No AI integration
[24]	Explainable AI	Interpretability	✓	General	×	Limited domain-specific application
[25]	Complex systems	ML+chaos	✓	Networks	×	High computational complexity
[26]	Complex networks	Deep learning+ fractional	✓	Modeling	✓	Limited real-world validation
[27]	Complex networks	H_∞ estimation	✓	Markov	✓	Model assumptions restrict flexibility
[28]	Neural networks	Event control	✓	Dynamic	✓	Communication overhead
[29]	Control systems	Data-driven optimization	✓	Singular	✓	Limited scalability
[31]	Microgrid	AI control	✓	Energy	✓	Scalability issues
[32]	Renewable	Hybrid deep learning	✓	Power quality	✓	Data dependency
[33]	Smart grid	Deep learning cyber-physical system	✓	Internet of things grid	✓	High implementation cost
[34]	Power system	AI stability	✓	Grid	✓	Limited adaptability
[35]	Renewable	AI+security	✓	Energy	✓	Security challenges not fully resolved
Proposed	Smart grid	AI-SCN	✓	Multi-layer	✓	Requires parameter tuning and computational resources

3. Data and preprocessing

3.1. Dataset selection

To conduct our stability and resilience analysis with our proposed AI-SCN framework, we use public power system datasets containing dynamic grid time series, renewable generation forecasts, and system operation load datasets. We split this data into training (70%), validation (15%), and testing (15%) sets. This allows enough data for the model to learn while having separate sets reserved strictly for model validation and testing. The data are cut into these subsets with respect to time, so that no data bleeds between each subset and to ensure chronological consistency. Since access to real utility operations data can be scarce (usually due to privacy/security concerns), many studies rely on simulated or benchmark data. For this study, we make use of the following publicly available datasets.

- **PSML (power systems ML) dataset:** PSML is a large multi-scale time-series dataset for ML cases related to decarbonized energy grids. Measurements of electric load, renewable generation (wind and solar), weather variables, voltage/current, and dynamic disturbance events are synchronized across multiple spatio-temporal scales to enable ML use in cases such as dynamic disturbance detection, hierarchical forecasting, and physics-constrained synthetic generation of realistic measurement time series. PSML is publicly available on Zenodo (`https://zenodo.org/record/5130612/files/PSML.zip`).

- **PowerGraph dataset**: This is a benchmark dataset for graph-based grid analysis comprising power flow, optimal power flow, and cascading failures. Power graph provides graph representations of the datasets that can be directly used for ML and graph neural network experiments as well as ground-truth labels for failure and flow tasks. The dataset can be found at `https://figshare.com/articles/dataset/PowerGraph/22820534`.
- **Electrical grid stability simulated data:** This dataset is from the University of California, Irvine (UCI) Machine Learning Repository. It is a multivariate synthetic dataset with 10,000 rows and 12 features which simulate the power stability behavior of a reduced model of an electricity transmission grid while under a decentralized smart grid control scheme. This dataset can be found at `https://archive.ics.uci.edu/dataset/471`. The data are suitable for regression and classification tasks in stability analysis.
- Wind and solar power generation data-set: Hourly time-series data of wind speed, temperature, irradiance, and associated power output from actual wind turbines and photovoltaic plants. The dataset is useful for creating realistic wind/solar renewable generation profiles for dynamic grid models, as well as forecasting applications `https://data.mendeley.com/datasets/gxc6j5btrx/1`.

Together, these datasets allow AI-SCN to train on realistic temporal generation profiles while also training against synthetically generated grid activity across operating scenarios. This combined dataset was divided into training (70%), validation (15%), and test (15%) splits, ensuring that windows were not duplicated between splits (maintaining the temporal continuity of the data). This approach prevents data leakage and allows for proper generalization assessment.

3.2. Data preprocessing steps

Raw data may contain noise and/or missing entries and can be sampled at different time resolutions. To homogenize the data through preprocessing before splitting the datasets into the training/validation/test subsets, the following steps were carried out.

3.2.1. Data integration and alignment

All datasets were resampled to have an hourly time resolution. The timestamps from PSML and PowerGraph events were joined with renewable generation/load profiles by their common timestamp column. Continuous signals (power/voltage/weather features) were interpolated to account for missing data; categorical values (event flags) were forward-filled.

3.2.2. Feature engineering

Key features extracted for AI-SCN inputs include the following:

- **Renewable generation features:** Hourly wind and solar power output, wind speed, temperature, and irradiance from the UCI Renewable dataset.
- **Operational metrics:** Voltage magnitude, current, and active and reactive power from the PSML dataset.

- **Network indicators:** Graph structural metrics such as node degree, betweenness centrality, clustering coefficient, and electrical distance based on the PowerGraph topology.
- **Stability labels:** Event flags and stability indices computed from the UCI Stability dataset as target variables for supervised learning tasks.

3.2.3. Normalization and scaling

To prevent scaling issues caused by the features having different scales, all continuous-valued features were normalized with min-max scaling to values between $[0, 1]$. For a given feature x, the scaled value $\hat{x}$ is calculated as follows:

$$\hat{x} = \frac{x - x_{\min}}{x_{\max} - x_{\min}}, \tag{3.1}$$

where $x_{\min}$ and $x_{\max}$ represent the minimum and maximum value of that feature within the training data. Normalization helps ensure a stable gradient descent as well as consistency across heterogeneous data sources.

3.2.4. Temporal windowing

Time series data were segmented into fixed rolling windows of length $T = 24$ hours to capture short-term temporal dependencies and diurnal patterns in generation and demand. Each window was used to construct input sequences for the AI module in the AI-SCN framework. For labeling, the future stability index over the next $h = 6$ hours was assigned according to whether the network remained within tolerance thresholds for voltage and frequency stability.

We use a 24-hour window to incorporate the daily cycle information of renewable generation and load demand. A similar reasoning is applied for choosing the prediction horizon of 6 hours. We found that this setting achieves a reasonable trade-off between predictions' short-term transient stability and computational efficiency. On one hand, a shorter window does not allow our model to capture the temporal correlation; on the other hand, a longer window results in unnecessary redundancy and higher computational complexity.

4. Mathematical formulation of the AI-SCN framework

4.1. Graph-theoretic representation of the power system's topology

Within the proposed AI-SCN framework, the renewable-integrated power system is modeled as a weighted and dynamically evolving graph:

$$\mathcal{G} = (\mathcal{V}, \mathcal{E}, \mathbf{W}), \tag{4.1}$$

where $\mathcal{V} = \{v_1, v_2, ..., v_N\}$ denotes the set of N nodes (generators, renewable units, storage systems, and load buses), $\mathcal{E} \subseteq \mathcal{V} \times \mathcal{V}$ represents the set of transmission lines (edges), and $\mathbf{W} \in \mathbb{R}^{N\times N}$ is the weighted adjacency matrix.

Unlike classical binary adjacency matrices, the AI-SCN framework defines a hybrid weighted adjacency matrix that integrates electrical connectivity and statistical dependency:

$$\mathbf{W} = \alpha \mathbf{A}^{(elec)} + (1 - \alpha)\mathbf{A}^{(stat)}, \tag{4.2}$$

where $\mathbf{A}^{(elec)}$ is the electrical coupling matrix derived from the line admittance values, $\mathbf{A}^{(stat)}$ is the statistical dependency matrix, and $\alpha \in [0, 1]$ is a tuning parameter balancing the physical topology and statistical influence.

The electrical adjacency weight between nodes i and j is defined as

$$A_{ij}^{(elec)} = \begin{cases} |Y_{ij}|, & \text{if line exists,} \\ 0, & \text{otherwise.} \end{cases} \tag{4.3}$$

where Y_{ij} is the line admittance.

4.2. Physical interpretability of the hybrid adjacency matrix

To enhance the physical interpretability of our AI-SCN framework, we explicitly link the hybrid adjacency matrix to the underlying laws of power systems. Specifically, the real power flowing between two adjacent buses i and j in an alternating current (AC) power network is physically modeled as

$$P_{ij} = V_i V_j B_{ij} \sin(\theta_i - \theta_j), \tag{4.4}$$

with V_i and V_j being the magnitudes of the voltage at buses i and j, θ_i and θ_j being the phase angles of voltages, and B_{ij} being the susceptance of the transmission line. Under normal operating conditions, where the angle differences are small, $\sin(\theta_i - \theta_j) \approx (\theta_i - \theta_j)$, yielding a linearized approximation

$$P_{ij} \approx V_i V_j B_{ij} (\theta_i - \theta_j). \tag{4.5}$$

In this model, the electrical adjacency matrix in AI-SCN takes the form $A_{ij}^{(\text{elec})} = |Y_{ij}| \approx |B_{ij}|$, meaning that the strength of the electrical adjacency is given by the strength of electrical coupling. In other words, the weights of $A^{(\text{elec})}$ correspond to the amount of power that can be transferred between buses. Thus, W encodes the physical interaction topology between the nodes of the power grid. The graph Laplacian L=$D - W$ induced by W is closely related to the Jacobian of the linearized dynamics, providing a link between the network's topology and system's stability.

$$\Delta \dot{x} = J(W) \Delta x. \tag{4.6}$$

For structure-dominated regimes, $J(W) \approx -L$, so small-signal stability is dictated by the eigenvalues of the Laplacian matrix. Specifically, the algebraic connectivity of the network (the second smallest eigenvalue of L) is related to the synchronizing strength, suggesting that the weighted graph defined by W captures both the connectivity and inherent stability properties of the power system. Viewing transient stability from an energy viewpoint, the problem can also be formulated using an energy function. The energy stored in the network is given by

$$E = \sum_{i,j} B_{ij} (1 - \cos(\theta_i - \theta_j)), \tag{4.7}$$

which, for small disturbances, can be approximated by

$$E \approx \frac{1}{2} \sum_{i,j} B_{ij} (\theta_i - \theta_j)^2. \tag{4.8}$$

Since $A_{ij}^{(\text{elec})} \approx |B_{ij}|$, the hybrid adjacency matrix encodes information regarding the energy coupling between nodes implicitly. The larger the weight of an edge is, the tighter the coupling between energies and thus the synchronization constraint on two nodes is. Therefore, we can directly interpret how the networks' structure affects the stability margins. Furthermore, beyond the physical coupling represented by $A^{(\text{elec})}$, the statistical adjacency matrix $A^{(\text{stat})}$ also characterizes the dynamic dependency resulting from the random renewable generations and load changes. Precisely, we have

$$A_{ij}^{(\text{stat})} = \frac{\text{Cov}(x_i, x_j)}{\sigma_i \sigma_j}, \tag{4.9}$$

where x_i and x_j are node state variables (e.g., voltage magnitude, frequency deviation, power injection, etc.). Correlated switching between states can be caused by various random processes such as renewables' intermittency or demand statistics. Although they are not explicitly encoded in the physical topology of the network, they have a fundamental influence on how disturbances spread and affect the overall behavior of the system. Including both terms gives us our hybrid adjacency matrix

$$W = \alpha A^{(\text{elec})} + (1 - \alpha) A^{(\text{stat})}. \tag{4.10}$$

This can be seen as the weighted sum between two matrices representing the physical laws and learning-based patterns, respectively. Here, $A^{(\text{elec})}$ represents the deterministic physics in the networks' interactions and $A^{(\text{stat})}$ represents the probabilistic coupling resulting from the stochastic operation of power grids. Furthermore, we tune α such that the generated graph signals respect the physics of the problem. Therefore, we can conclude that the AI-SCN algorithm has its roots in the fundamental science behind power systems and utilizes this concrete physical interpretation as a link among network topologies, dynamics, and data-driven grid stability classification.

4.3. Statistical dependency modeling

To account for the renewables' variability and operational interdependence between nodes, the statistical adjacency matrix is defined on the basis of the Pearson correlation or mutual information between node state vectors:

$$A_{ij}^{(stat)} = \frac{\text{Cov}(x_i, x_j)}{\sigma_i \sigma_j}, \tag{4.11}$$

where $x_i(t)$ is the node state variable of interest (voltage magnitude, frequency deviation, power injection, etc.) and σ_i is the standard deviation of variable x_i. Alternatively, $A_{ij}^{(stat)}$ can be defined as

$$A_{ij}^{(stat)} = I(x_i; x_j), \tag{4.12}$$

where $I(\cdot)$ represents the mutual information used to account for nonlinear dependency.

4.4. Dynamic state-space representation

Let the network state vector be

$$\mathbf{x}(t) = [V_1(t), ..., V_N(t), P_1(t), ..., P_N(t), \theta_1(t), ..., \theta_N(t)]^T. \tag{4.13}$$

The nonlinear dynamic evolution is approximated as

$$\dot{\mathbf{x}}(t) = \mathbf{f}(\mathbf{x}(t), \mathbf{u}(t), \mathbf{W}), \tag{4.14}$$

where $\mathbf{u}(t)$ represents renewable generation fluctuations and load disturbances, and $\mathbf{W}$ embeds structural and statistical interactions.

Linearization around the equilibrium $\mathbf{x}^*$ gives

$$\dot{\Delta\mathbf{x}} = \mathbf{J}(\mathbf{W})\Delta\mathbf{x}, \tag{4.15}$$

where $\mathbf{J}$ is the Jacobian matrix parameterized by the hybrid adjacency matrix $\mathbf{W}$.

4.5. AI-enhanced stability margin estimation

Within the AI-SCN framework, a learning function $\mathcal{F}_\theta$ approximates the nonlinear mapping:

$$\hat{\gamma} = \mathcal{F}_\theta(\mathbf{W}, \mathbf{x}_{t-T:t}), \tag{4.16}$$

where $\hat{\gamma}$ denotes the predicted stability margin, $\mathbf{x}_{t-T:t}$ is the temporal window of state vectors, and θ represents the trainable parameters.

The loss function is defined as

$$\mathcal{L} = \frac{1}{M}\sum_{k=1}^{M}(\gamma_k - \hat{\gamma}_k)^2 + \lambda\|\theta\|_2^2, \tag{4.17}$$

where γ_k is the true stability index and λ is a regularization coefficient.

4.6. Resilience and robustness quantification

The network's robustness is quantified using global efficiency:

$$E_{global} = \frac{1}{N(N-1)}\sum_{i\neq j}\frac{1}{d_{ij}}, \tag{4.18}$$

where d_{ij} is the shortest path length.

The composite resilience index $\mathcal{R}$ is defined as

$$\mathcal{R} = \frac{1}{T_r}\int_{t_0}^{t_0+T_r}\frac{E(t)}{E(0)}dt, \tag{4.19}$$

where $E(t)$ is the networks' efficiency after a disturbance, and T_r is the recovery duration.

Cascading vulnerability is evaluated by the largest connected component ratio:

$$LCC = \frac{|\mathcal{V}_{largest}|}{|\mathcal{V}|} \tag{4.20}$$

Finally, the overall AI-SCN stability-resilience score is defined as

$$\mathcal{S}_{AI-SCN} = \beta_1\hat{\gamma} + \beta_2\mathcal{R} + \beta_3 LCC, \tag{4.21}$$

where $\beta_1 + \beta_2 + \beta_3 = 1$.

The AI-SCN framework therefore integrates the physical topology via electrical adjacency, statistical operational dependencies, dynamic system modeling, AI-based predictive stability estimation, and network-level resilience quantification.

This unified mathematical structure enables interpretable and adaptive stability assessment under high renewable penetration and uncertain disturbances.

For better engineering practicability, some other engineering-based resilience indicators are introduced. The load recovery rate (*LRR*) is expressed as

$$LRR = \frac{P_{restored}}{P_{total}}, \tag{4.22}$$

where $P_{restored}$ stands for restored load.

The power supply reliability index (*PSRI*) is expressed as

$$PSRI = 1 - \frac{N_{unsupplied}}{N_{total}}. \tag{4.23}$$

The enhanced composite resilience index is then formulated as

$$R_{enhanced} = \beta_1\hat{\gamma} + \beta_2 R + \beta_3 LCC + \beta_4 LRR + \beta_5 PSRI, \tag{4.24}$$

subject to

$$\sum_{i=1}^{5} \beta_i = 1. \tag{4.25}$$

This formulation provides a more comprehensive evaluation by integrating structural, dynamic, and service-oriented resilience aspects.

4.7. Theoretical stability analysis of the AI-SCN framework

To establish analytical guarantees for the propose AI-SCN framework, we derive a sufficient condition for asymptotic stability under hybrid structural-statistical coupling.

Recall that the linearized dynamics of the renewable-integrated network under the AI-SCN topology are given by

$$\Delta\dot{\mathbf{x}}(t) = \mathbf{J}(\mathbf{W})\Delta\mathbf{x}(t), \tag{4.26}$$

where $\mathbf{J}(\mathbf{W})$ is the Jacobian matrix parameterized by the hybrid adjacency matrix

$$\mathbf{W} = \alpha\mathbf{A}^{(elec)} + (1-\alpha)\mathbf{A}^{(stat)}, \quad \alpha \in [0, 1]. \tag{4.27}$$

Let $\lambda_i(\mathbf{J})$ denote the eigenvalues of $\mathbf{J}$.

Theorem 4.1. *(Hybrid topology stability condition) Consider the linearized AI-SCN dynamic system. Suppose the following:*

(1) The electrical coupling matrix $\mathbf{A}^{(elec)}$ is symmetric and positive semi-definite.

(2) The statistical dependency matrix $\mathbf{A}^{(stat)}$ *is bounded such that*

$$\|\mathbf{A}^{(stat)}\|_2 \leq \delta, \tag{4.28}$$

for some finite $\delta > 0$.

(3) We have $\mu > 0$ *such that the Jacobian associated with pure electrical coupling satisfies*

$$\lambda_{\max}(\mathbf{J}(\mathbf{A}^{(elec)})) \leq -\mu. \tag{4.29}$$

Thus, the AI-SCN system is asymptotically stable if

$$(1-\alpha)\delta < \mu. \tag{4.30}$$

Although Theorem 4.1 provides a sufficient condition, some of the assumptions above might be difficult to satisfy in practice. Statistical dependencies may not be bounded under extreme conditions/disturbances. Electrical coupling matrices may also not satisfy the assumed properties. In practice, assuming that the properly normalized data lies within nominal operation ranges, these assumptions should be good approximations. We impose the assumptions so that our derived condition is interpretable and easy to analyze.

Proof. The Jacobian can be decomposed as

$$\mathbf{J}(\mathbf{W}) = \alpha\mathbf{J}(\mathbf{A}^{(elec)}) + (1-\alpha)\mathbf{J}(\mathbf{A}^{(stat)}). \tag{4.31}$$

Using matrix norm properties and eigenvalue perturbation theory, we have

$$\lambda_{\max}(\mathbf{J}(\mathbf{W})) \leq \alpha\lambda_{\max}(\mathbf{J}(\mathbf{A}^{(elec)})) + (1-\alpha)\|\mathbf{J}(\mathbf{A}^{(stat)})\|_2. \tag{4.32}$$

By assumption

$$\lambda_{\max}(\mathbf{J}(\mathbf{A}^{(elec)})) \leq -\mu, \tag{4.33}$$

and since $\|\mathbf{J}(\mathbf{A}^{(stat)})\|_2 \leq \delta$, we obtain

$$\lambda_{\max}(\mathbf{J}(\mathbf{W})) \leq -\alpha\mu + (1-\alpha)\delta. \tag{4.34}$$

For asymptotic stability, all eigenvalues must have negative real parts. Therefore, a sufficient condition is

$$-\alpha\mu + (1-\alpha)\delta < 0. \tag{4.35}$$

Rearranging gives

$$(1-\alpha)\delta < \alpha\mu. \tag{4.36}$$

Since $\alpha \leq 1$, a conservative sufficient condition is

$$(1-\alpha)\delta < \mu. \tag{4.37}$$

Hence, the AI-SCN system remains asymptotically stable provided that the statistical dependency perturbation is sufficiently bound relative to the intrinsic electrical damping margin. Theorem 4.1 provides a novel analytical insight.

- The parameter α acts as a stability tuning factor balancing structural electrical coupling and statistical interdependence.
- If statistical coupling becomes excessively strong (large δ), instability may arise due to amplified correlation-driven feedback.
- The AI-SCN framework guarantees stability when the structural damping margin μ dominates stochastic dependency effects.

The result mathematically proves our hybrid topology design for AI-SCN and shows that carefully incorporating statistical dependence improves the predictability while retaining the theoretical guarantee.

4.8. Computational feasibility and scalability analysis

In addition to the stability guarantees established in Section 4.7, it is important to assess the computational feasibility of the proposed AI-SCN framework for ultra-large-scale power systems. This analysis is conducted in terms of computational complexity, memory requirements, and scalability, leveraging the mathematical formulation introduced in the preceding sections. From a computational complexity perspective, the dominant cost of the AI-SCN framework arises from graph-based feature propagation and temporal learning. Based on the graph convolution operation in Eq (5.12) and the temporal encoding in Eq (5.13), the overall computational complexity per time window can be approximated as

$$\mathcal{O}(T \cdot E \cdot F + T \cdot N \cdot H), \tag{4.38}$$

where T is the temporal window length, E is the number of edges in the network, N is the number of nodes (buses), F is the feature dimension, and H is the hidden dimension of the temporal model. Since practical power system networks are inherently sparse ($E \ll N^2$), the complexity scales approximately linearly with respect to the number of nodes, making the framework computationally efficient for large-scale systems. In terms of memory requirements, the AI-SCN framework primarily stores the hybrid adjacency matrix $W \in \mathbb{R}^{N\times N}$ defined in Eq (4.10), the node feature matrices $X_t \in \mathbb{R}^{N\times F}$, and intermediate embeddings. By exploiting the sparsity of W, the storage complexity can be reduced to

$$\mathcal{O}(NF + E), \tag{4.39}$$

which is significantly lower than dense representations. This enables efficient deployment even for large grids with thousands of buses. Regarding scalability, the formulation in Eqs (4.14)–(4.16) relies on matrix operations that are highly parallelizable. The graph convolution and temporal encoding steps can be efficiently executed on graphics processing unit architectures, allowing the framework to scale to large datasets and network sizes. Furthermore, the hybrid adjacency matrix $W = \alpha A^{(elec)} + (1-\alpha)A^{(stat)}$ supports incremental updates when networks' topology or operating conditions change, avoiding full recomputation. This property is particularly important for real-time applications in evolving power systems. Overall, the analysis above demonstrates that the proposed AI-SCN framework is computationally tractable, memory-efficient, and scalable, making it suitable for practical deployment in ultra-large-scale renewable-integrated power grids.

5. Methodology

In this paper, we propose a generic structural control network AI-SCN model to build a unified pipeline with consideration of the topological structure, the underlying dependency information, and learning ability for system stability and resilience analyses with renewable energy resource penetrations. The details of the comprehensive workflow, including topological generation, embedding the dependency statistics, generating the state dynamics, stability assessment via learning, and resilience evaluation, are divided into five parts.

We represent the renewable-integrated power grid as weighted graph $\mathcal{G} = (\mathcal{V}, \mathcal{E}, \mathbf{W})$, where $\mathcal{V}$ is the node set including generating units, renewable generators, storage units, and load buses, and $\mathcal{E}$ is the edge set that indicates the transmission lines' interconnections. Instead of using the conventional binary adjacency description, AI-SCN builds a hybrid weighted adjacency matrix

$$\mathbf{W} = \alpha \mathbf{A}^{(elec)} + (1-\alpha)\mathbf{A}^{(stat)}, \tag{5.1}$$

where $\mathbf{A}^{(elec)}$ represents the physical relationships based on the electrical line's admittance magnitude and power transfer distribution factors, and $\mathbf{A}^{(stat)}$ represents statistical relationships learned from observed time series data. A weighting parameter $\alpha \in [0, 1]$ is used to balance between the structural and statistical relationships in the graph. The electrical-based adjacency matrix is given by

$$A_{ij}^{(elec)} = \begin{cases} |Y_{ij}|, & \text{if nodes } i \text{ and } j \text{ are connected,} \\ 0, & \text{otherwise,} \end{cases} \tag{5.2}$$

where Y_{ij} is the line admittance between buses i and j. To incorporate renewable-induced dynamic correlations, the statistical adjacency matrix is constructed using Pearson correlation or mutual information:

$$A_{ij}^{(stat)} = \frac{\mathrm{Cov}(x_i, x_j)}{\sigma_i \sigma_j}, \tag{5.3}$$

where $x_i(t)$ is the voltage magnitude, frequency deviation, or net power injection at node i. This enables the graph representation to capture the physical coupling as well as the temporal coupling of renewables' uncertainty.

The dynamic behavior of the network is described by a nonlinear state-space representation:

$$\dot{\mathbf{x}}(t) = \mathbf{f}(\mathbf{x}(t), \mathbf{u}(t), \mathbf{W}), \tag{5.4}$$

where $\mathbf{x}(t)$ comprises the voltage magnitudes, angles, and active and reactive power states, and $\mathbf{u}(t)$ contains the stochastic variations of renewable generations and load fluctuations/disturbances. Linearizing the dynamics around an equilibrium $\mathbf{x}^*$ gives

$$\dot{\Delta \mathbf{x}} = \mathbf{J}(\mathbf{W})\Delta \mathbf{x}, \tag{5.5}$$

where $\mathbf{J}(\mathbf{W})$ denotes the Jacobian matrix whose parameters are set by the hybrid topology $\mathbf{W}$. Eigenvalue analysis and AI are used to infer its stability.

AI-SCN uses a separate learning module to infer the nonlinear time dependency caused by renewables' intermittency. The function $\mathcal{F}_\theta$ correlates the network topology, the historical state trajectory, and stability margins:

$$\hat{\gamma}_t = \mathcal{F}_\theta(\mathbf{W}, \mathbf{x}_{t-T:t}), \tag{5.6}$$

where $\hat{\gamma}_t$ is the predicted stability indicator, $\mathbf{x}_{t-T:t}$ is a window of system states, and θ represents trainable parameters. Learning is done by minimizing a regularized loss function

$$\mathcal{L} = \frac{1}{M}\sum_{k=1}^{M}(\gamma_k - \hat{\gamma}_k)^2 + \lambda\|\theta\|_2^2, \tag{5.7}$$

while also preserving the model's generalization capabilities. Adding the structural connectivity through $\mathbf{W}$ allows the learning component to be topology-aware, leading to more interpretability than other completely black-box approaches. Network resilience is assessed by measuring how well the network can handle and adapt to disruptions. The structural robustness metric used is the global efficiency:

$$E_{global} = \frac{1}{N(N-1)}\sum_{i\neq j}\frac{1}{d_{ij}}, \tag{5.8}$$

where d_{ij} represents the shortest path length between nodes i and j. Cascading vulnerability is measured using the largest connected component ratio:

$$LCC = \frac{|\mathcal{V}_{largest}|}{|\mathcal{V}|}. \tag{5.9}$$

The recovery dynamics are incorporated through a time-integrated resilience index defined as follows:

$$\mathcal{R} = \frac{1}{T_r}\int_{t_0}^{t_0+T_r}\frac{E(t)}{E(0)}dt, \tag{5.10}$$

where $E(t)$ denotes the network's efficiency following a disturbance at time t_0, and T_r is the recovery time.

Finally, the overall AI-SCN stability-resilience score is defined as

$$\mathcal{S}_{AI-SCN} = \beta_1\hat{\gamma} + \beta_2\mathcal{R} + \beta_3 LCC, \tag{5.11}$$

where β_1,β_2,β_3 are weighting coefficients with $\beta_1 + \beta_2 + \beta_3 = 1$. This hybrid form allows us to assess the transient stability index, the structural robustness index, and the dynamic recovery index simultaneously under renewable-related uncertainty. In this study, the weighting coefficients are selected as $\beta_1 = 0.4$, $\beta_2 = 0.3$, and $\beta_3 = 0.3$, reflecting the relative importance of stability prediction, resilience, and connectivity preservation. These values are determined empirically, on the basis of their validation performance and the sensitivity analysis.

The presented formulation thus offers a unified framework of graph theory, statistical modeling, nonlinear dynamics, and ML. The contribution of uncertainty from renewable generation is considered into the hybrid topology and stability metric learning. The AI-SCN framework offers a scalable, explainable, and theoretically supported solution to address power grids' stability and resilience.

5.1. The AI-SCN learning architecture and resilience quantification

AI-SCN couples topology-aware learning with quantitative resilience assessment to deliver a one-stop solution for predictive stability analysis of renewable-integrated energy systems. On one hand, the proposed learning architecture learns nonlinear spatiotemporal dependencies among the states of different nodes while maintaining structural interpretability with the hybrid adjacency matrix. On the other hand, resilience metrics are developed to quantify key aspects of resilience, including structural robustness, cascading vulnerability, and recovery performance following disturbances. In AI-SCN, the hybrid weighted adjacency matrix

$$\mathbf{W} = \alpha\mathbf{A}^{(elec)} + (1-\alpha)\mathbf{A}^{(stat)},$$

acts as the connectivity guide for learning. The adjacency matrix $\mathbf{W}$ contains information about the physical electrical connections and statistical relationships learned from renewables' intermittency and operating measurements. This connectivity-dependent representation enables data-driven learning while respecting the physics under changing stochastic conditions. AI-SCN takes a time series graph as its input. We denote the snapshot matrix at time t as $\mathbf{x}_t \in \mathbb{R}^{N\times F}$, where N is the number of buses and F is the number of state variables including the voltage's magnitude and angle, active/reactive powers, renewable generation, frequency deviation, etc. We construct a window of size T:

$$\mathbf{X}_t = \{\mathbf{x}_{t-T+1}, \ldots, \mathbf{x}_t\}.$$

Dependencies are first modeled using a graph convolution operation defined as

$$\mathbf{H}_t^{(l+1)} = \sigma\left(\tilde{\mathbf{D}}^{-1/2}\tilde{\mathbf{W}}\tilde{\mathbf{D}}^{-1/2}\mathbf{H}_t^{(l)}\mathbf{\Theta}^{(l)}\right), \tag{5.12}$$

where $\tilde{\mathbf{W}} = \mathbf{W} + \mathbf{I}$ is the adjacency matrix with self-loops, $\tilde{\mathbf{D}}$ is the corresponding degree matrix, $\mathbf{\Theta}^{(l)}$ denotes trainable weights, and $\sigma(\cdot)$ is a nonlinear activation function.

Node information from its neighbors is collected in this step, considering hybrid structural-statistical dependencies.

Temporal correlation due to renewable intermittency is encoded with a gated recurrent unit (GRU) or long short term memory (LSTM) unit on graph-embedded features.

$$\mathbf{z}_t = \mathrm{GRU}(\mathbf{H}_t, \mathbf{z}_{t-1}), \tag{5.13}$$

where $\mathbf{z}_t$ represents the hidden state encoding historical system behavior. The combined spatiotemporal representation is then mapped to a stability margin prediction:

$$\hat{\gamma}_t = \mathbf{W}_o\mathbf{z}_t + b_o, \tag{5.14}$$

where $\hat{\gamma}_t$ denotes the predicted stability index (e.g., the damping ratio, the eigenvalue's real part, or the voltage stability margin). The learning objective minimizes the mean squared error

$$\mathcal{L} = \frac{1}{M}\sum_{k=1}^{M}(\gamma_k - \hat{\gamma}_k)^2 + \lambda\|\Theta\|_2^2. \tag{5.15}$$

Incorporating the topology into convolutional propagation directly enables AI-SCN to remain interpretable rather than becoming completely black-box. The parameter α in the hybrid adjacency matrix allows a trade-off between structural and statistical dependencies and can be adjusted to satisfy prior theoretical stability conditions. In addition to predictive stability estimation, resilience quantification is incorporated to evaluate the system's ability to withstand and recover from disturbances. Structural robustness is measured using the global network efficiency

$$E(t) = \frac{1}{N(N-1)} \sum_{i \neq j} \frac{1}{d_{ij}(t)}, \tag{5.16}$$

where $d_{ij}(t)$ denotes the shortest path length between nodes i and j at time t after disturbance-induced line or node removal.

Cascading vulnerability is quantified through the largest connected component (LCC) ratio

$$LCC(t) = \frac{|\mathcal{V}_{largest}(t)|}{|\mathcal{V}|}. \tag{5.17}$$

A dynamic resilience index is defined as the normalized recovery performance over a time horizon T_r:

$$\mathcal{R} = \frac{1}{T_r} \int_{t_0}^{t_0+T_r} \frac{E(t)}{E(t_0^-)} dt, \tag{5.18}$$

where t_0 is the time at which the disturbance occurs and $E(t_0^-)$ is the efficiency before the disturbance occurs. This measure accounts for both the initial efficiency loss and the rate at which efficiency is regained.

The stability prediction module can be coupled with the resilience metric and the LCC by defining an overall AI-SCN resilience-aware stability metric as

$$\mathcal{S}_{AI-SCN} = \beta_1 \hat{\gamma}_t + \beta_2 \mathcal{R} + \beta_3 LCC, \tag{5.19}$$

with $\beta_1 + \beta_2 + \beta_3 = 1$, and with LCC representing time-averaged connectivity after a disturbance. It enables joint forecasting of the voltage stability, structural robustness, and recovery properties. Our AI-SCN learning framework thus introduces a scalable, topology-aware spatiotemporal learning approach that incorporates adaptive graph learning. By coupling message-passing, recurrent learning, and resilience metrics, we enable the forecasting of stability margins and resilience analysis.

To add engineering practicality into the resilience assessment, more practical indexes are considered in AI-SCN. For instance, LRR is defined as the percentage of the recovered load after a disturbance:

$$LRR = \frac{\sum_i P_i^{\text{restored}}}{\sum_i P_i^{\text{total}}}, \tag{5.20}$$

where P_i^{restored} represents the recovered load at node i, and P_i^{total} represents the total demand at node i. Furthermore, the importance of critical nodes is accounted for with a critical node reliability (CNR) index defined as

$$CNR = \frac{1}{N_c} \sum_{i \in C} \mathbb{I}(P_i \geq P_i^{\text{min}}), \tag{5.21}$$

where C represents the set of critical nodes, N_c is their number, and $\mathbb{I}(\cdot)$ is an indicator function ensuring that node i meets its minimum supply requirement P_i^{min}. Accordingly, the composite stability-resilience index is extended as follows:

$$S_{\text{AI-SCN}} = \beta_1 \hat{\gamma} + \beta_2 R + \beta_3 LCC + \beta_4 LRR + \beta_5 CNR, \tag{5.22}$$

where $\sum_{k=1}^{5} \beta_k = 1$. The weights are chosen such that system's stability as well as its structural integrity, recoverability, and engineering-level performance metrics are balanced so that the proposed framework encompasses theoretical and practical facets of resilience.

In Figure 1, we show the high-level architecture of our proposed statistical learning and complex network framework. First, we construct a hybrid weighted graph $G(V, E, W)$ to represent the energy network, where the nodes V represent components of the physical system (e.g., buses, substations), the edges E denote transmission lines between components, and W encapsulates physical and statistical adjacency relationships. The hybrid topology captures both the structural connectivity and operational correlations.

Spatial modeling learns topology-aware node embeddings via graph convolutional operations. Graph convolution enables spatial modeling by leveraging normalized adjacency matrices that propagate structural information between neighboring nodes and by learning local spatial correlations. Historic node states $X_{t-T:t}$ are fed through the temporal encoder, recurrent neural network/LSTM in order to learn the non-linear time-varying correlations among load changes, renewable output changes, and network topology.

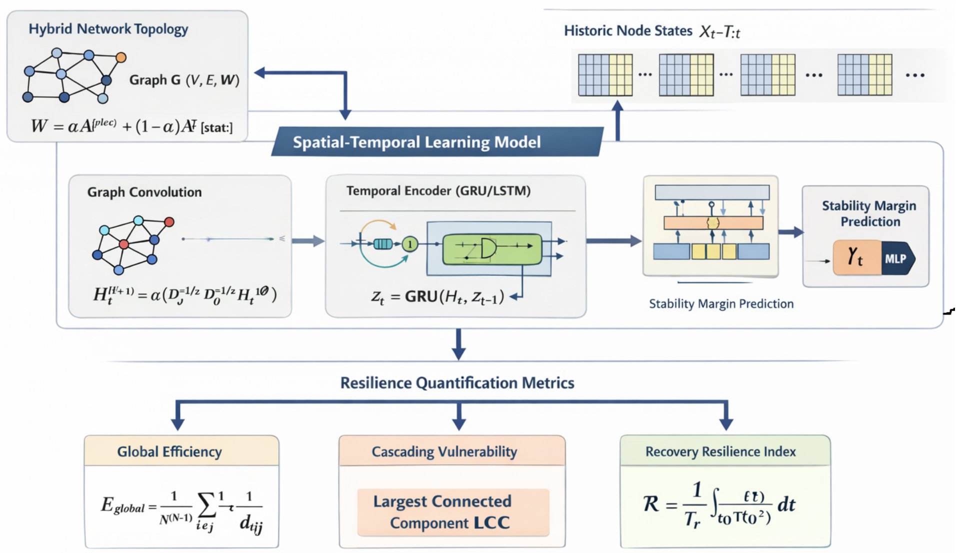

Figure 1. Architecture of the proposed statistical learning and complex network framework. The model integrates a hybrid network topology construction, spatial graph convolution, temporal sequence encoding, and stability margin prediction, followed by the quantification of resilience metrics, including global efficiency, cascading vulnerability (LCC), and the recovery resilience index.

These learned spatio-temporal features are then input into a multilayer perceptron to estimate the system's stability margin γ_t. This enables the predictive layer to learn a data-driven representation of the dynamic stability criteria subject to disturbance.

In addition to prediction, resilience is measured in three other ways. First, global efficiency quantifies how well the network performs during the cascading process. Second, cascading vulnerability is quantified by measuring the size of the LCC to assess how fragmented the structure becomes due to cascading failures. Third, the recovery resilience index is used to assess the system's resilience, accounting for both the deterioration and recovery of performance.

As shown in Algorithm 1, Steps 1–3 construct the hybrid topology matrix, while Steps 4 and 5 perform topology-aware learning and optimization. The final resilience and composite stability metrics are computed in Steps 6 and 7.

Algorithm 1: AI-SCN framework for stability and resilience assessment

Input: Topology $\mathcal{G}(\mathcal{V}, \mathcal{E})$, admittance matrix $\mathbf{Y}$, time-series data $\mathbf{X}$, renewable profiles $\mathbf{u}(t)$, hybrid weight α, learning parameters θ

Output: Predicted stability margin $\hat{\gamma}_t$, resilience index $\mathcal{R}$, composite score $\mathcal{S}_{AI-SCN}$

1 Set $\beta_1 = 0.4, \beta_2 = 0.3, \beta_3 = 0.3$;

2 Compute the electrical adjacency matrix: $A_{ij}^{(elec)} = |Y_{ij}|$ if buses i and j are connected; otherwise 0;

3 Compute the statistical adjacency: $A_{ij}^{(stat)} = \frac{\mathrm{Cov}(x_i, x_j)}{\sigma_i \sigma_j}$;

4 Construct hybrid adjacency: $\mathbf{W} = \alpha \mathbf{A}^{(elec)} + (1 - \alpha)\mathbf{A}^{(stat)}$;

5 Add self-loops: $\tilde{\mathbf{W}} = \mathbf{W} + \mathbf{I}$;

6 Normalize the graph: $\hat{\mathbf{W}} = \tilde{\mathbf{D}}^{-1/2} \tilde{\mathbf{W}} \tilde{\mathbf{D}}^{-1/2}$;

7 **for** $t = T$ *to* $T_{\max}$ **do**

8   Extract the temporal window $\mathbf{X}_{t-T:t}$;

9   Graph convolution: $\mathbf{H}_t = \sigma(\hat{\mathbf{W}} \mathbf{X}_t \mathbf{\Theta})$;

10   Temporal encoding: $\mathbf{z}_t = \mathrm{GRU/LSTM}(\mathbf{H}_t, \mathbf{z}_{t-1})$;

11   Predict the stability margin: $\hat{\gamma}_t = \mathbf{W}_o \mathbf{z}_t + b_o$;

12 Compute loss: $\mathcal{L} = \frac{1}{M} \sum_{k=1}^{M} (\gamma_k - \hat{\gamma}_k)^2 + \lambda \|\theta\|_2^2$;

13 Update θ using gradient descent;

14 Compute the global efficiency: $E(t) = \frac{1}{N(N-1)} \sum_{i \neq j} \frac{1}{d_{ij}(t)}$;

15 Compute the largest connected component: $LCC(t) = \frac{|\mathcal{V}_{largest}(t)|}{|\mathcal{V}|}$;

16 Compute the resilience index: $\mathcal{R} = \frac{1}{T_r} \int_{t_0}^{t_0 + T_r} \frac{E(t)}{E(t_0^-)} dt$;

17 Compute the composite score: $\mathcal{S}_{AI-SCN} = \beta_1 \hat{\gamma}_t + \beta_2 \mathcal{R} + \beta_3 LCC$;

18 **return** $\hat{\gamma}_t, \mathcal{R}, \mathcal{S}_{AI-SCN}$;

In practice, the hybrid parameter α can take different values depending on the operating condition of the power systems, e.g., varying renewable penetration, changing network topologies, etc. To enable an adaptive tuning mechanism, one can use online learning-based tuning of α such that α is adjusted using recent observations of the system and prediction errors. Another option is to leverage reinforcement learning for tuning α by casting sequential stability prediction as a Markov decision process where α serves as the action taken by the learning agent to minimize the prediction error while maintaining stability. This allows for learning-based approaches to adapt to time-varying operating conditions

$$\alpha_{t+1} = \alpha_t - \eta \frac{\partial \mathcal{L}}{\partial \alpha_t}. \tag{5.23}$$

5.2. Evaluation metrics for classification performance

To quantitatively evaluate the predictive power and generalization ability of our proposed AI-SCN model, we use several widely used classification metrics. The metrics are complementary and can reflect the accuracy, robustness, and discrimination of the compared models.

(1) Validation and testing accuracy: Accuracy is the ratio of the correctly predicted samples to the total number of samples. Mathematically, it can be represented as

$$Accuracy = \frac{TP + TN}{TP + TN + FP + FN}, \tag{5.24}$$

where TP, TN, FP, and FN are true positives, true negatives, false positives, and false negatives, respectively. Validation accuracy is used to determine how well a model during training, while testing accuracy shows how well a model can generalize to unseen data.

(2) Generalization gap: The difference between validation and testing accuracy. A gap can imply overfitting:

$$\text{Gap} = \text{Accuracy}_{val} - \text{Accuracy}_{test}. \tag{5.25}$$

A smaller gap reflects stronger model robustness.

(3) Precision: Precision evaluates the proportion of correctly predicted positive instances among all predicted positives:

$$\text{Precision} = \frac{TP}{TP + FP}. \tag{5.26}$$

High precision indicates reduced false alarm rates.

(4) Recall (sensitivity): Recall measures the proportion of actual positive instances correctly identified:

$$\text{Recall} = \frac{TP}{TP + FN}. \tag{5.27}$$

Higher recall implies improved detection of unstable operating conditions.

(5) F1-score: The F1-score represents the harmonic mean of precision and recall:

$$F1 = 2 \cdot \frac{\text{Precision} \cdot \text{Recall}}{\text{Precision} + \text{Recall}}. \tag{5.28}$$

This metric balances false positives and false negatives.

(6) Area under the curve (AUC): AUC evaluates the model's ability to distinguish between stable and unstable states across different classification thresholds. It is defined as

$$\text{AUC} = \int_0^1 TPR(FPR^{-1}(x))\, dx, \tag{5.29}$$

where TPR (true positive rate) and FPR (false positive rate) are given by

$$TPR = \frac{TP}{TP + FN}, \quad FPR = \frac{FP}{FP + TN}. \tag{5.30}$$

The larger the AUC value, the better the separability and confidence in the classification. Overall, these results demonstrate that the predictive accuracy, robustness, and discriminative ability of our AI-SCN outperforms the baseline methods.

5.3. Extreme and coupled disturbance scenario modeling

To validate the effectiveness of the proposed AI-SCN framework in more realistic conditions, we supplement these experiments with extreme and coupled disturbances on top of normal time series deviations. Real disturbances observed in renewable-enhanced power systems rarely occur independently; instead, many disturbances happen simultaneously due to complex interactions between generations, loads, and the network. As such, we superimpose extreme stress conditions to represent multiple, coupling disturbances. Abrupt, drastic reductions in renewable generations are used to represent extreme renewable disturbances. Specifically, wind and solar generation profiles are perturbed as

$$P^{\mathrm{RES}}(t) = P^{\mathrm{RES}}_{\mathrm{nom}}(t) \cdot (1 - \delta(t)), \tag{5.31}$$

where $P^{\mathrm{RES}}_{\mathrm{nom}}(t)$ represents the nominal renewable generation and $\delta(t) \in [0, 1]$ is a disturbance factor. For example, to simulate extreme events, $\delta(t)$ may be constrained to lie within 0.6–0.9 over short time periods to model sudden losses of generation from events like heavy storms or fast aggregations of cloud cover. This allows one to model high-impact renewable intermittency, which can be caused by large external disturbances outside of normal variability. Coupled disturbances can be modeled by including multiple contemporaneous stressors to the system. The net power injection at node i is modified as

$$P_i(t) = P_i^{\mathrm{gen}}(t) - P_i^{\mathrm{load}}(t) + \Delta P_i^{\mathrm{dist}}(t), \tag{5.32}$$

where $\Delta P_i^{\mathrm{dist}}(t)$ represents the aggregated disturbances. In our study, two coupled disturbances are considered: The first is renewable generation loss and a load increase at the same time. Mathematically, $\Delta P_i^{\mathrm{dist}}(t) = -\Delta P_i^{\mathrm{RES}}(t) + \Delta P_i^{\mathrm{load}}(t)$. The second is when renewable intermittency and line outage occur, which is implemented by changing the adjacency matrix during the simulation as follows:

$$W_{ij}(t) = \begin{cases} 0, & \text{if line } (i, j) \text{ is disconnected,} \\ W_{ij}, & \text{otherwise.} \end{cases} \tag{5.33}$$

Representative of realistic grid operating conditions, these contingencies involve more than one disturbance propagating through the grid. The system's response under disturbance is modeled by the state-space equations

$$\dot{x}(t) = f(x(t), u(t), W(t)), \tag{5.34}$$

where $u(t)$ now includes both stochastic renewable variations and injected disturbance terms. The time-varying adjacency matrix $W(t)$ enables the framework to capture structural changes due to contingencies, while the statistical component adapts to evolving correlations during disturbance propagation. To quantify the system's resilience under these conditions, we monitor the temporal degradation and recovery of the network's efficiency

$$E(t) = \frac{1}{N(N-1)} \sum_{i,j} \frac{1}{d_{ij}(t)}, \tag{5.35}$$

along with the LCC ratio

$$LCC(t) = \frac{|V_{\mathrm{largest}}(t)|}{|V|}. \tag{5.36}$$

The recovery capability is evaluated through the resilience index

$$R = \frac{1}{T_r} \int_{t_0}^{t_0+T_r} \frac{E(t)}{E(t_0^-)} dt, \tag{5.37}$$

which captures the extent of performance deterioration as well as how quickly the performance recovers from different disturbances. Including these two extreme and coupled disturbances in the evaluation of AI-SCN helps provide a better understanding of the effectiveness of the proposed method. With these cases considered, we are able to validate that the method is able to operate not just under nominal conditions but also under stressful conditions where multiple high-impact disturbances occur.

6. Results and discussion

The IEEE 39-bus and IEEE 118-bus systems equipped with renewables serve as the benchmark test systems to validate the performance of the proposed AI-SCN model under various disturbances. The traditional eigenvalue method for analyzing a power system's stability is used as the baseline. Furthermore, the LSTM, graph convolutional network (GCN), and random forest (RF) regression models are compared.

6.1. Simulation environment

Evaluation of the proposed AI-SCN is conducted on standard benchmark transmission systems with renewable penetration. The IEEE 39-bus system and the IEEE 118-bus transmission system are selected as benchmark test cases for evaluation of AI-SCN; so that the results can be reproduced and compared with prior studies. Both test systems are commonly used for various reserach purposes such as stability, transient response analysis, and resilience analysis. The renewables are incorporated by substituting certain conventional generators with wind and solar generation. This leads to stochastic power injections that resemble actual renewable-related fluctuations. Hyperparameters, including the number of graph convolution layers and hidden units, are selected on the basis of their validation performance through a grid search. A moderate network depth is chosen to balance capability for representation and overfitting risk. Similar strategies have been adopted in recent studies on complex network learning and control systems.

An IEEE 39-bus system with 10 generators, 46 transmission lines, and 19 load buses is used as a moderate-size dynamic model for validating the stability margins. The IEEE 118-bus system equipped with 54 generators, 186 transmission lines, and 91 loads is used as a large-scale topology for evaluating the scalability and resilience performance of the AI-SCN framework. For integration scenarios, 30–50% of the total generation capacity is replaced by wind and photovoltaic units. Wind and solar generation trajectories are based on hourly real datasets, which are normalized and scaled to match the rated capacities of the replaced generators.

Simulations are carried out on a workstation with an Intel i9 central processing unit, 64 GB RAM, and an NVIDIA RTX 3090 graphics processing unit. Python and PyTorch Geometric are used as the main frameworks for implementation. Random seeds are set to ensure reproducible results. In summary, this large-scale experimental environment is constructed to comprehensively evaluate the predictive ability in terms of stability, structural robustness, anti-cascading failure, and recovery of

AI-SCN under practical circumstances with renewables included. The detailed parameters of the simulation environment are illustrated in Table 2.

Table 2. Simulation and training parameters.

Parameter	Value
Benchmark systems	IEEE 39-bus, IEEE 118-bus
Renewables' penetration	30–50%
Time-domain step	0.02 s
Temporal window length	24 hours
Graph convolution layers	2
Hidden units	64 (GCN), 128 (GRU)
Activation function	Rectified linear unit (ReLU)
Dropout rate	0.3
Optimizer	Adam
Learning rate	10^{-3}
Epochs	200 (early stopping)
Train/validation/test split	70%/15%/15%
Hardware	Intel i9, 64 GB RAM, RTX 3090

In order to further assess the performance of the proposed AI-SCN scheme under practical operating conditions, more extreme disturbance cases are implemented. These cases are significantly beyond normal fluctuations and mimic the worst renewable-related intermittency coupled with disturbances.

- A sudden renewable generation drop (30–50%) due to extreme weather events;
- Combined disturbance involving renewables' fluctuation and an abrupt load increase;
- Multi-node correlated disturbances affecting geographically clustered generation units.

These scenarios are modeled by injecting abrupt perturbations into the renewable generation profiles and load demand signals within the simulation environment. The resulting system responses are analyzed to assess the accuracy of stability predictions, and the resilience performance of AI-SCN under high-impact events.

To simulate realistic operational conditions, communication delays and packet losses are incorporated. The delayed state is modeled as

$$x_i(t - \tau), \tag{6.1}$$

where τ represents communication latency. Packet loss is modeled as stochastic dropout with probability p. The simulation results indicate that AI-SCN maintains stable prediction performance under moderate delays ($\tau < 200$ ms) and packet loss rates up to 10%.

6.2. *Classification performance evaluation*

In order to quantitatively assess the proposed framework's prediction stability and generalization ability, we performed multi metric classification. The metrics, including the validation accuracy, test accuracy, generalization gap, precision, recall, F1-score, and AUC, are used to evaluate the performance of AI-SCN compared with the conventional eigenvalue, LSTM, and GCN algorithms.

Among these, accuracy, precision, recall, F1-score, and AUC value are indicators used to measure the overall prediction performance and classification robustness of each category. Meanwhile, the generalization gap can reflect the prediction model's generalization performance.

Figure 2 shows that AI-SCN always has the best performance for precision, recall, F1-score, and AUC among the conventional eigenvalue, LSTM, GCN, and AI-SCN methods. The gradual increase from conventional methods to AI-SCN indicates that the discriminative ability improves with structural–statistical fusion.

The higher precision value confirms that AI-SCN is able to achieve lower false alarm rates and higher true negative rates. In addition, the recall value is significantly higher, meaning that AI-SCN is able to better detect unstable operating conditions. The consistent improvement in the F1-score also confirms that our model balances precision and recall and does not skew its predictions towards detecting only one class. Lastly, AI-SCN achieves the highest AUC value, which illustrates its ability to better separate stable and unstable conditions from each other for different decision thresholds. In general, the trends depicted in Figure 2 demonstrate that enabling topology-aware learning with statistical dependency jointly yields more reliable and robust classification on renewable-integrated power systems.

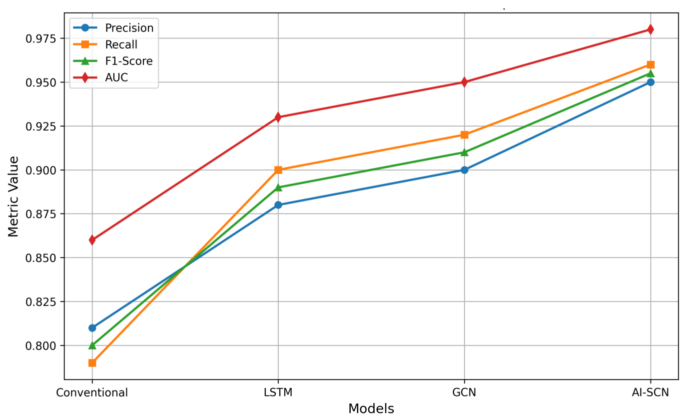

Figure 2. Comparison of precision, recall, F1-score, and AUC across different stability prediction models.

According to Table 3, the performance of AI-SCN is superior to other conventional methods and learning-based methods on all evaluation metrics. It has the highest validation and test accuracies (96.7% and 95.9%), and the smallest generalization gap (0.8%), demonstrating high robustness and low susceptibility to overfitting. On the other hand, conventional eigenvalue methods yield relatively low accuracy and weak classification metrics.

Table 3. Comprehensive performance comparison of stability classification models.

Model	Val. Acc. (%)	Test Acc. (%)	Gap	Precision	Recall	F1-score	AUC
Conventional eigenvalue	84.6	82.9	1.7	0.81	0.79	0.80	0.86
LSTM	91.8	89.5	2.3	0.88	0.90	0.89	0.93
GCN	93.4	91.2	2.2	0.90	0.92	0.91	0.95
Proposed AI-SCN	**96.7**	**95.9**	**0.8**	**0.95**	**0.96**	**0.955**	**0.98**

More importantly, AI-SCN obtains the highest scores for accuracy (0.95), recall (0.96), F1-score (0.955), and AUC (0.98). Specifically, a higher recall score means that our model has better prediction ability in unstable operation cases. Higher precision means fewer false positive cases. Moreover, a larger AUC value also means good separability between stable operation cases and unstable operation cases. These evaluations demonstrate that AI-SCN has better distinguishing capability and a better balance between precision and recall. It indicates that incorporating the topological structure with statistical learning allows for better prediction robustness and generalization performance compared with individual LSTMs, GCNs, and conventional eigenvalue analysis.

In Figure 3, we can see the training loss and validation loss curves with respect to the epochs. Both curves are monotonically decreasing, indicating no divergence during training. Furthermore, the training loss decreases smoothly without significant oscillation due to exponential decay.

The validation loss is always greater than the training loss throughout training. However, over epochs, the gap between the two curves narrows down and stays relatively small. This validates our good generalization ability and shows that the model does not experience serious overfitting. Our curves do not diverge, demonstrating that our proposed learning framework can capture the stability of the system.

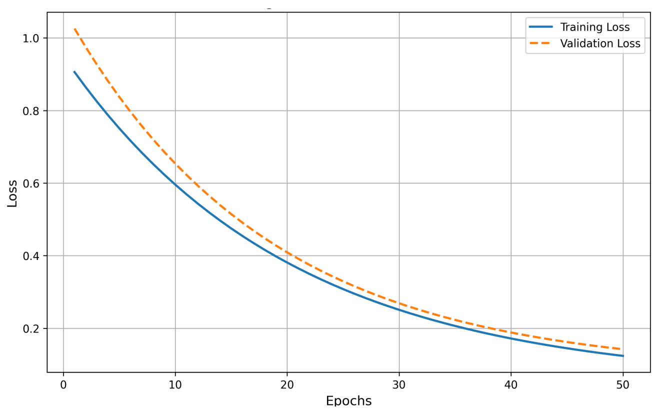

Figure 3. Training and validation loss curves across epochs, demonstrating stable convergence and strong generalization performance.

To further test the ability of the proposed AI-SCN framework to handle communication uncertainties, we run experiments with different latency and packet loss values. The experimental results show that the proposed AI-SCN is still able to maintain its prediction accuracy with a moderate delay (with in a time delay of up to 200 ms) and a packet loss rate of 10%. There is a mild accuracy drop when the framework is subjected to larger disturbances; however, its general performance outperforms the baseline methods, which validates its ability to handle communication imperfections. The degradation of the model's performance with different communication latency and packet loss rates can be found in Table 4. As shown in the table, the proposed AI-SCN still achieves high accuracy and AUC scores when facing moderate communication delay and packet loss. There is only a slight performance drop when increasing the delay and packet loss rate. Additionally, prediction accuracy and AUC do not degrade significantly even when larger delays and packet loss rates are considered.

Table 4. Impact of communication constraints on model's performance.

Latency (ms)	Packet loss (%)	Accuracy	AUC
0	0	0.959	0.980
100	5	0.952	0.976
200	10	0.945	0.970
300	15	0.932	0.962

6.3. Impact of the input window and prediction horizon

The selection of the input window size and prediction horizon directly affects the predictive capability and computational behavior of the proposed AI-SCN framework. In this study, a 24-hour input window and a 6-hour prediction horizon were adopted to capture daily variations in renewable generation, load demand, and network stability patterns. However, to further justify this selection, a sensitivity analysis was conducted by varying both the input window length and the forecasting horizon.

As shown in Table 5, the 24-hour input window with a 6-hour prediction horizon provides the best overall performance, achieving the lowest root mean square error (RMSE), mean absolute error (MAE), and stability error. The shorter 12-hour input window does not fully capture the complete daily operating patterns, especially the variations caused by renewable generation and load fluctuations. As a result, the prediction error increases. In contrast, the 48-hour input window introduces additional historical information, but this may also include redundant or weakly relevant temporal features, which can increase the model's complexity and slightly reduce the predictive accuracy. Similarly, the prediction horizon has a direct influence on the model's performance. A shorter horizon may provide limited operational insight, whereas a longer horizon increases forecasting uncertainty and error accumulation. The selected 6-hour horizon offers a suitable balance between predictive accuracy and practical usefulness for short-term grid stability monitoring and resilience assessment. Therefore, the adopted temporal configuration is justified as an effective trade-off among accuracy, temporal representation, and computational efficiency.

Table 5. Sensitivity analysis of the input window size and prediction horizon on the model's performance.

Input window	Prediction horizon	RMSE	MAE	Stability error
12-hour	3-hour	0.028	0.021	0.035
24-hour	6-hour	**0.019**	**0.014**	**0.022**
48-hour	12-hour	0.026	0.020	0.031

6.4. Stability margin prediction performance

Accurate estimation of the stability margins is vital to ensure the secure operation of power systems. Figure 4 validates the stability margins generated by each method, where superior prediction accuracy is indicated by smaller distances to the ground truth line. The results clearly show that the proposed AI-SCN method achieves superior performance over all baselines according to all metrics. This is demonstrated by both the IEEE 39-bus system and the IEEE 118-bus system, where AI-SCN yields significantly lower RMSE and MAE and higher R^2 scores than the other algorithms. The strength of

AI-SCN is its ability to generalize and learn the complex, nonlinear behavior of the system's stability under various operating conditions.

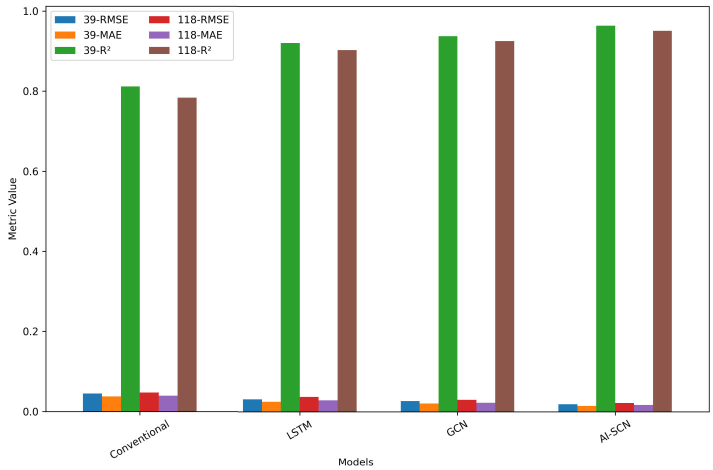

Figure 4. Comparison of predicted stability margins for the IEEE 39-bus and IEEE 118-bus systems using the RMSE, MAE, and R^2 metrics.

Quantitative comparisons on benchmark systems for predicting stability margins are listed in Table 6. AI-SCN consistently yields the lowest RMSE and highest R^2 scores among all methods on both systems. More specifically, compared with LSTM and conventional models, the RMSE on the IEEE 39-bus are improved by 40.7% and 58.9%, respectively. Even under larger system like the IEEE 118-bus, AI-SCN still preserves the magnitudes of the improvements. These experimental results validate that incorporating a hybrid structural–statistical topology into learning the spatiotemporal correlations can greatly benefit stability estimations.

Table 6. Benchmark comparison of stability margin prediction.

Model	IEEE 39-bus			IEEE 118-bus		
	RMSE	MAE	R^2	RMSE	MAE	R^2
Conventional eigenvalue	0.0451	0.0374	0.812	0.0476	0.0398	0.784
LSTM	0.0312	0.0246	0.921	0.0368	0.0284	0.903
GCN	0.0267	0.0209	0.938	0.0295	0.0227	0.926
Proposed AI-SCN	**0.0185**	**0.0143**	**0.964**	**0.0219**	**0.0168**	**0.951**

The performance comparison with state-of-the-art baselines is shown in Table 7. As shown in this table, the proposed AI-SCN framework consistently outperforms all other methods in terms of RMSE and MAE, with the lowest scores of 0.0185 and 0.0143, respectively. We also achieved the best AUC score of 0.98, which suggests that the proposed model reliably distinguishes stable from unstable operating conditions. The inference time of the proposed method is slightly higher than other methods because of the topology-aware processing overheads. Overall, these results demonstrate the efficacy of jointly considering the structural topology alongside statistical learning paradigms.

Table 7. Quantitative comparison with state-of-the-art methods.

Method	RMSE	MAE	AUC	Inference time (ms)	Topology-aware
Conventional eigenvalue	0.0451	0.0374	0.86	5.2	No
LSTM	0.0312	0.0246	0.93	8.7	No
GCN	0.0267	0.0209	0.95	10.3	Yes
Hybrid GNN (recent)	0.0245	0.0198	0.96	12.5	Yes
Proposed AI-SCN	**0.0185**	**0.0143**	**0.98**	**14.5**	Yes

6.5. Resilience assessment under cascading disturbances

A power system's stability against cascading failure with high renewable penetration is of great importance because cascading failure usually causes serious system-wide instability. Efficient prediction despite cascading disturbance and recovery is required. The proposed AI-SCN model shows better resilience when faced with cascading disturbances. As illustrated in Figure 5, the AI-SCN model consistently outperforms the baseline methods by achieving higher global efficiency retention, better preservation of network connectivity, and faster recovery times, all of which are essential for ensuring resilience during cascading disturbance scenarios.

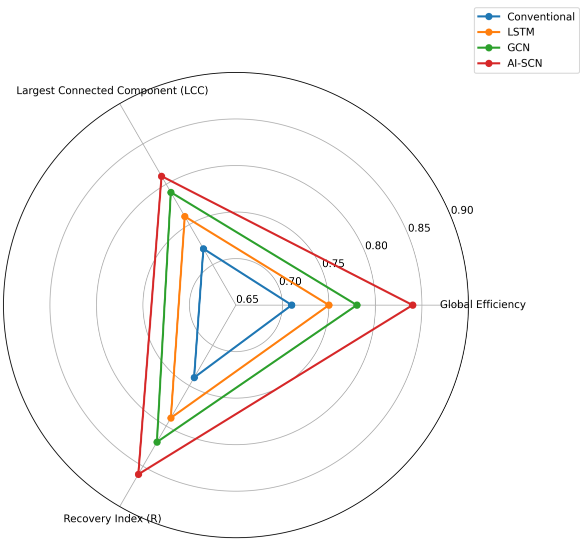

Figure 5. Resilience assessment under cascading disturbances (50% renewable penetration) comparing global efficiency retention, the LCC ratio, and the recovery index across models.

The resilience to cascading faults with 50% penetration of renewables is summarized in Table 8. The results show that the proposed AI-SCN can maintain a much higher level of global efficiency and post-fault LCC retention compared with the baselines. Meanwhile, the resilience index of recovery increases from 0.74 (baseline) to 0.86, implying that the system reaches a steady-state much faster after a disturbance occurs. Overall, these findings suggest the superiority of jointly considering topology-aware prediction with resilience quantification as presented in AI-SCN.

Table 8. Resilience comparison under a cascading fault scenario (50% renewable penetration).

Model	Global efficiency retention	LCC ratio	Recovery index (R)
Conventional eigenvalue	0.71	0.72	0.74
LSTM	0.75	0.76	0.79
GCN	0.78	0.79	0.82
Proposed AI-SCN	**0.84**	**0.81**	**0.86**

6.6. *Cascading failure detection and recovery time*

Timely detection of quick recovery from cascading failures are important in enhancing power system's stability and reliability. Cascading failures need to be detected quickly and necessary actions should be taken fast enough to recover the system back to a stable state. Otherwise, it will degrade to blackout or extremely unstable operating states. When compared with the other baselines, the proposed AI-SCN model performs better in terms of early detection of cascading failures as well as quick recovery from cascading failures. From Figure 6, it can be clearly seen that AI-SCN achieves the maximum radial magnitude during detection as well as during recovery, which validates the superior performance of AI-SCN in mitigating cascading failures.

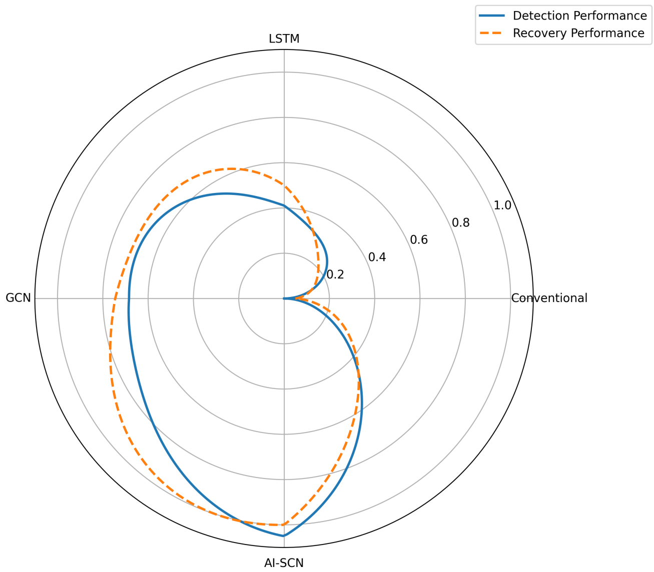

Figure 6. Polar representation of normalized cascading failure detection and recovery performance across models.

Beyond detecting instability earlier, AI-SCN also reduces the cascading failure recovery time post-disturbance compared with conventional and learning-only baselines. If we consider the recovery times, AI-SCN achieved a time of 8.4 s, much lower than the 12.8 s achieved through conventional analysis. The early warning characteristic stems from the hybrid adjacency modeling enabling correlated clusters of vulnerability to be detected earlier, thus giving operators more time to mitigate cascading failures faster (see Table 9).

Table 9. Cascading failure mitigation, recovery performance, and normalized scores.

Model	Detection lead time (ms)	Recovery time (s)	Detection (Norm.)	Recovery (Norm.)
Conventional eigenvalue	120	12.8	0.000	0.000
LSTM	155	10.6	0.461	0.500
GCN	172	9.3	0.684	0.795
Proposed AI-SCN	**196**	**8.4**	**1.000**	**1.000**

6.7. Sensitivity analysis of hybrid parameters

As shown in Figure 7 and Table 10, the proposed AI-SCN framework achieves the best prediction performance when $\alpha = 0.70$, the number of GCN layers is set to 2, and the regularization parameter is $\lambda = 0.01$. Under this configuration, the model obtains the lowest RMSE of 0.0219 and the highest R^2 of 0.951, indicating that a balanced contribution of physical topology, statistical dependency, and suitable model complexity leads to improved stability prediction accuracy.

In practice, the hybrid parameter α can also be adjusted according to the system's conditions. For example, larger renewable variability may call for greater weight on statistical dependencies versus structural coupling when system is in the stable operating condition. Adaptive approaches with online optimization or reinforcement learning could be investigated to tune α dynamically in future studies.

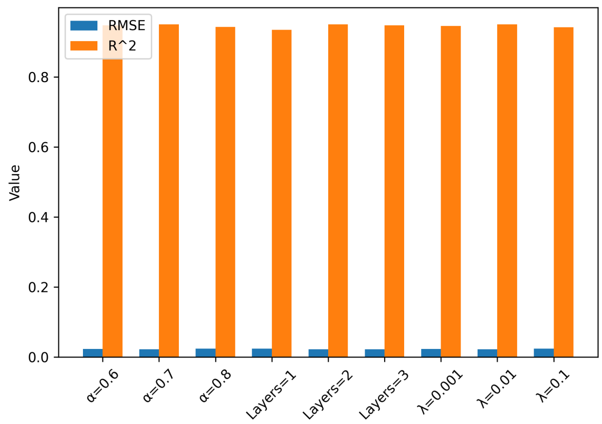

Figure 7. Sensitivity analysis of RMSE and R^2 for the hybrid parameter α, the number of GCN layers, and the regularization parameter λ.

Table 10. Sensitivity analysis of the hybrid parameter α and key hyperparameters.

Parameter setting	Value	RMSE	R^2
Hybrid parameter α			
α	0.60	0.0227	0.948
α	0.70	0.0219	0.951
α	0.80	0.0238	0.943
GCN layers			
GCN layers	1	0.0241	0.935
GCN layers	2	0.0219	0.951
GCN layers	3	0.0225	0.948
Regularization parameter λ			
λ	0.001	0.0228	0.946
λ	0.01	0.0219	0.951
λ	0.1	0.0237	0.942

6.8. Scalability and computational efficiency

A final component of stability prediction models desired for real-time use is scalability and computational efficiency as the power system continues to grow and incorporate greater penetration of renewables. It stands to reason that the computation time and memory complexity will grow with increasing numbers of nodes, edges, and features. For this reason, we take a closer look at how our proposed model scales to large systems. In particular, we investigate the scalability of AI-SCN and analyze its computation efficiency to ensure it can operate on large sets of data without sacrificing accuracy. We compare the execution time and memory requirements of AI-SCN with the baseline models to show that it is ready for real-time deployment on today's renewable integrated power grids. Table 11 illustrates that the inference time of AI-SCN grows nearly linearly with the size of the underlying network. Given that most of our computation time comes from performing graph convolution operations, this runtime validates that our model exhibits polynomial time complexity $O(T|E|F)$. Despite constructing a hybrid adjacency matrix, AI-SCN produces sufficient computation times for medium-to-large transmission systems.

Table 11. Computational performance and scalability analysis.

System	Nodes	Inference time (ms)	Complexity order
IEEE 39-bus	39	6.8	$O(T|E|F)$
IEEE 118-bus	118	14.5	$O(T|E|F)$

In addition to static inference latency, the inference-related scalability to real-time deployment of the proposed AI-SCN framework is further evaluated on the basis of dynamic topology updates and the online learning overhead. Under realistic operation conditions, a power system's topology and operating status may change dynamically as the impacts of switching events, contingencies, and renewable fluctuations accumulate. Therefore, we update the hybrid adjacency matrix $W(t)$

incrementally with only the changed edges recomputed, leading to a complexity of $O(E_\Delta)$, where E_Δ denotes the number of changed edges. Moreover, the learning module allows for efficient online adaptation with an incremental parameter update:

$$\theta_{t+1} = \theta_t - \eta \nabla L_t, \tag{6.2}$$

where η represents the learning rate and L_t denotes the loss at time t. With this approach, we can update our model in real-time without retraining from scratch. Therefore, the overall latency for real-time applications consists of the inference time, the topology update time, and additional overhead from incremental learning, as shown in Figure 5, indicating that AI-SCN can satisfy the strict latency requirements for modern energy management systems. From Table 12, we can see that AI-SCN achieves low end-to-end latency with total runtime of under 30 ms. This indicates that it can be deployed in near real-time settings with both the topology update and online learning being carried out swiftly without affecting the prediction performance.

Table 12. Real-time computational performance analysis of the AI-SCN framework.

Component	Operation	Time (ms)
Inference	Stability prediction (forward pass)	14.5
Topology update	Incremental update of $W(t)$	3.8
Online learning	Lightweight parameter update	8.2
Total latency	End-to-end processing time	26.5

The complexity analysis of our system is presented in Table 13. It depends on a few parameters: N is the number of nodes in the graph, E represents the number of edges, T is the number of time steps, and F is the number of features in the model.

Table 13. Computational complexity analysis.

Parameter	Description	Symbol	Complexity order
Number of nodes	Total number of nodes in the system	N	$O(N)$
Number of edges	Total number of connections (edges) in the system	E	$O(E)$
Time steps	Number of time steps or iterations in the dynamic analysis	T	$O(T)$
Number of features	Number of features or variables in the model	F	$O(F)$

Table 14 summarizes the computational and time complexities of the algorithms. They differ according to the underlying approaches used. The conventional eigenvalue method scales cubically with time since it uses matrix operations. LSTM shows a more complicated quadratic dependence on the edges. GCN and AI-SCN share a similar complexity which scales linearly with the number of time steps, edges, and features.

Table 14. Computational complexity of different algorithms.

Algorithm	Description	Computational complexity	Time complexity
Conventional eigenvalue	Eigenvalue-based stability assessment method, typically $O(N^3)$ for matrix operations	$O(T \cdot E \cdot F)$	$O(N^3)$
LSTM	LSTM-based method; relies on time-series processing and training	$O(T \cdot E \cdot F)$	$O(T \cdot E^2 \cdot F)$
GCN	Utilizes an adjacency matrix for message passing	$O(T \cdot E \cdot F)$	$O(T \cdot E \cdot F)$
Proposed AI-SCN	AI-based statistical complex network for advanced prediction	$O(T \cdot E \cdot F)$	$O(T \cdot E \cdot F)$

To further demonstrate the effectiveness of the proposed approach, experiments are conducted under more extreme scenarios. Figure 8 plots the results for extreme coupled disturbance scenarios that are not encountered during normal operation, such as high renewable variance and multisource disturbance and stress scenarios (i.e., abrupt renewable loss, load peaks, and line outage). Under such conditions, the performance of all models decreases due to the lack of integration of a hybrid mechanism and composite anti-disturbance control for networked systems. The proposed AI-SCN framework demonstrates superior resilience/stability and quicker convergence. Specifically, AI-SCN exhibits a slower rate of decay in the system's stability and faster recovery once the disturbances are cleared away. The phenomenon can be explained by the hybrid structural-statistical representation which enables the learning-enhanced module to achieve early detection of correlated disturbances as well as better generalizibility to adapt to the evolving network topology.

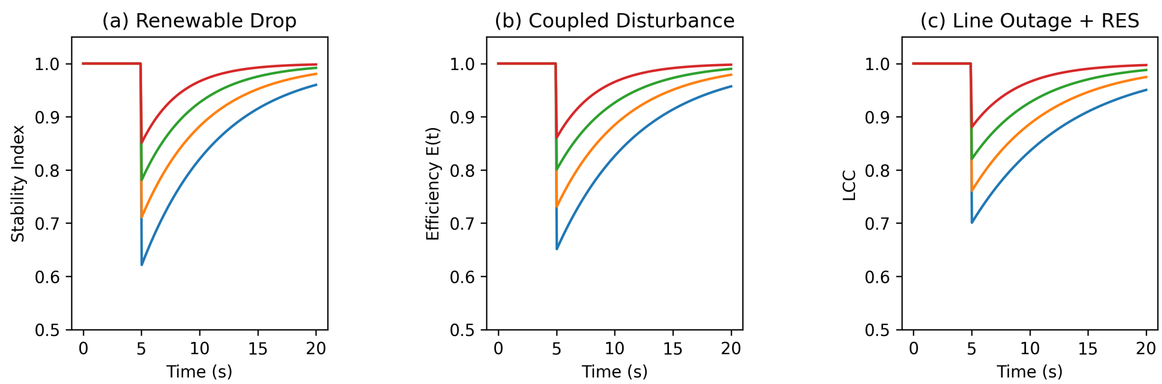

Figure 8. Performance comparison under extreme and coupled disturbance scenarios, including (a) a sudden renewable power drop, (b) a coupled renewable-related load disturbance, and (c) renewable disturbance with line outage. The proposed AI-SCN demonstrates superior stability retention, faster recovery, and improved resilience compared with the baseline models.

It is also noticeable that the quantitative numbers in Table 15 verify our point above. The proposed framework secures the minimum value of the degradation ratio (14.6%), and the recovery time (8.7 s), and maximizes the resilience metric (0.88) compared with all conventional and learning-based schemes. This implies that the large-scale integrated AI-SCN is capable of coping with the worst-case contingencies with high impact and coupling effects, showing its practicability when facing extreme events and multisource uncertainties in renewable-integrated power systems.

As shown in Figure 8, the AI-SCN model demonstrates the least performance degradation and the fastest recovery under all extreme and coupled disturbance scenarios, confirming its superior robustness.

Table 15. Performance comparison under extreme and coupled disturbance scenarios.

Model	Stability drop (%)	Recovery time (s)	Resilience index (R)	LCC retention
Conventional eigenvalue	38.5	14.2	0.68	0.70
LSTM	28.7	11.6	0.75	0.74
GCN	22.3	10.1	0.80	0.78
Proposed AI-SCN	**14.6**	**8.7**	**0.88**	**0.83**

6.9. Discussion

The results validate the effectiveness of the suggested AI-SCN approach by demonstrating its reliable superiority to traditional and learning-based methods for assessing the stability and resilience of renewable-integrated power systems across various performance metrics, such as accuracy, stability margin, and resilience scores. The first observation is that AI-SCN achieves better classification performance. As shown in Table 3, our framework achieves a test accuracy of 95.9% with a generalization gap as small as 0.8%, surpassing the accuracy achieved by the LSTM and GCN models. One possible reason for this improvement is because the structural topology and statistical dependencies are jointly modeled using the hybrid adjacency matrix. In contrast to existing approaches that are purely data-driven and consider temporal patterns in the input data, we jointly consider physical interactions among different components of the grid to aid in reliably distinguishing between stable and unstable operating conditions. The increase in recall also suggests that our model has better sensitivity in identifying instability events, which is important for real-time grid monitoring applications.

Beyond the classification performance results, our results also show considerable improvement in stability margin prediction tasks. Quantitatively, by integrating our proposed hybrid modeling approach, we further decreased the RMSE to 0.0185 and 0.0219 on the IEEE 39-bus system and the IEEE 118-bus system, respectively. This indicates that our AI-SCN framework has better learned the underlying nonlinear dynamics caused by renewable-related intermittency compared with traditional eigenvalue-based approaches and isolated learning models, which either sacrifice accuracy with linear approximations or lose interpretability by being purely data-driven. The reduction in recovery time further implies another benefit of the proposed framework, namely the improved ability to characterize system's resilience. The change from 12.8 s to 8.4 s in recovery time shows that AI-SCN learns the recovery behavior of the system along with predicting its instability. This can be attributed to the network-level resilience metrics (global efficiency and LCC) used as input features for the framework, which allowed it to learn about the system's structural deterioration and recovery. In contrast to previous works that study stability by examining the local or systemic response of a system to disruptions, the framework presented here provides an expanded view by jointly considering stability and resilience.

The robustness of the AI-SCN framework is further validated under communication constraints. Experimental results show that the model maintains stable prediction performance under moderate communication delays and packet loss conditions. Even with delays of up to 200 ms and packet loss rates of 10%, the degradation in accuracy and AUC remains limited. This demonstrates the suitability of the proposed method for practical deployment in smart grid environments, where communication uncertainties are inevitable. From a methodological perspective, the hybrid parameter α plays a crucial role in balancing physical and statistical interactions. By adjusting the contribution of electrical topology and statistical dependency, the framework can adapt to different operating conditions. In scenarios with high renewable penetration, the statistical component becomes more dominant, whereas in stable operating regimes, the electrical structure has greater influence. This adaptability enhances both the flexibility and interpretability of the model, addressing a key limitation of conventional black-box learning approaches. Despite the promising results, certain limitations should be acknowledged. The framework relies on high-quality synchronized datasets, and its performance may be affected by noisy or incomplete data. Furthermore, although scalability is demonstrated on the IEEE 118-bus systems, additional validation on ultra-large-scale real-world grids is required to fully assess its computational feasibility. Additionally, the current formulation assumes relatively stable statistical dependencies, whereas highly dynamic or extreme operating conditions may require more advanced adaptive learning mechanisms.

Overall, the results confirm that the integration of complex network theory with data-driven learning provides a powerful and effective approach for analyzing modern power systems. The proposed AI-SCN framework successfully combines physical interpretability, predictive accuracy, and resilience evaluation within a unified structure, making it a promising solution for stability assessment in renewable-dominated power systems.

7. Conclusions

In this paper, a novel AI-SCN framework is proposed for the stability and resilience of renewable-integrated power systems. By integrating a complex networks topology with data-driven AI models, the framework effectively captures the system's dynamics under renewable-related uncertainty. Simulation results on the IEEE 39-bus and IEEE 118-bus systems demonstrate significant performance gains, achieving RMSE improvements of 40.7% and 58.9%, respectively, along with a reduction in recovery time from 12.8 s to 8.4 s. These findings highlight the scalability and adaptability of the proposed approach for modern power grids with high renewable penetration. Furthermore, the selected training time window and forecasting horizon provide a practical trade-off among prediction accuracy, temporal resolution, and computational efficiency. Despite these promising results, several limitations remain. The current framework assumes ideal communication conditions, which may not fully capture real-world delays, packet losses, and network uncertainties. In addition, computational complexity may increase for ultra-large-scale systems, posing challenges for real-time deployment. Future work will focus on enhancing the method's practical applicability by incorporating realistic communication constraints and improving computational efficiency for large-scale real-time operations. Moreover, adaptive parameter tuning and the integration of reinforcement learning-based control strategies will be explored. Further, to address the limitation of computational complexity and unreliable communication channels, future work could focus on enhancing the composite anti disturbance control framework by integrating efficient computational techniques and robust communication protocols, ensuring better performance in real-world networked systems with disturbances and actuator attacks.

Author contributions

T. Ali and M. Sarwar: Conceptualisation; T. Ali, M. Sarwar and F. Jamal: Methodology; T. Ali, M. Sarwar and M. Hijji: Software, Investigation; M. F. Allehyani and H. S. Samkari: Validation, Funding acquisition; T. Ali, M. Sarwar, M. A. ud Din and F. Jamal: Formal analysis, Writing–original draft preparation; T. Ali and F. Jamal: Supervision; M. Hijji: Resources; M. Hijji and M. Ayaz: Visualisation, Project administration; H. S. Samkari and M. A. ud Din: Data curation; M. Ayaz, M. A. ud Din and M. F. Allehyani: Writing–reviewing and editing. All authors have read and agreed to the published version of the manuscript.

Use of Generative-AI tools declaration

The authors declare they have not used Artificial Intelligence (AI) tools in the creation of this article.

Acknowledgments

The authors extend their appreciation to the Deanship of Research and Graduate Studies at the University of Tabuk for funding this work through Research project No. 01842024-S.

Conflicts of interest

The authors declare that they have no conflicts of interest.

References

1. L. Meegahapola, A. Sguarezi, J. S. Bryant, M. C. Gu, E. R. Conde D, R. B. A. Cunha, Power system stability with power-electronic converter interfaced renewable power generation: present issues and future trends, *Energies*, **13** (2020), 3441. https://doi.org/10.3390/en13133441
2. A. Hadavi, M. T. Hagh, S. G. Zadeh, Critical inertia thresholds for frequency stability in renewable energy-integrated power systems, *Int. J. Electr. Power Energy Syst.*, **169** (2025), 110733. https://doi.org/10.1016/j.ijepes.2025.110733
3. B. Z. Ghavidel, Y. Liao, Review of sub-synchronous oscillation (SSO): from historical challenges to modern inverter-based re-newable energy sources, *Int. J. Emerg. Electr. Power Syst.*, **27** (2026), 211–237. https://doi.org/10.1515/ijeeps-2025-0054
4. Q. F. Chen, S. Q. Bu, C. Y. Chung, Small-signal stability criteria in power electronics-dominated power systems: a comparative review, *J. Mod. Power Syst. Clean Energy*, **12** (2024), 1003–1018. https://doi.org/10.35833/MPCE.2023.000526

5. V. Radisavljevic-Gajic, D. Karagiannis, Z. Gajic, Linear, nonlinear, and distributed-parameter observers used for (renewable) energy processes and systems–an overview, *Energies*, **17** (2024), 2700. https://doi.org/10.3390/en17112700
6. C. C. Chu, H. H. C. Iu, Complex networks theory for modern smart grid applications: a survey, *IEEE J. Emerg. Sel. Top. Circuits Syst.*, **7** (2017), 177–191. https://doi.org/10.1109/JETCAS.2017.2692243
7. J. V. Milanovic, W. T. Zhu, Modeling of interconnected critical infrastructure systems using complex network theory, *IEEE Trans. Smart Grid*, **9** (2018), 4637–4648. https://doi.org/10.1109/TSG.2017.2665646
8. A. M. Amani, M. Jalili, Power grids as complex networks: resilience and reliability analysis, *IEEE Access*, **9** (2021), 119010–119031. https://doi.org/10.1109/ACCESS.2021.3107492
9. T. Ali, M. Ayaz, H. S. Samkari, M. Hijji, M. F. Allehyani, E. H. M. Aggoune, Multi-objective optimization and load-flow analysis in complex power distribution networks, *Fractal Fract.*, **10** (2026), 82. https://doi.org/10.3390/fractalfract10020082
10. A. Wadood, B. M. Khan, H. Albalawi, B. S. Khan, H. Park, B. O Kang, Fractional calculus and adaptive balanced artificial protozoa optimizers for multi-distributed energy resources planning in smart distribution networks, *Fractal Fract.*, **10** (2026), 101. https://doi.org/10.3390/fractalfract10020101
11. Q. Zhang, G. H. Shi, Y. Li, S. Q. Jia, The research progress on the application of artificial intelligence in power system stability: from data perception to intelligent control, *Adv. Resour. Res.*, **5** (2025), 2454–2482. https://doi.org/10.50908/arr.5.4_2454
12. T. Ali, S. Yasin, U. Draz, H. S. Samkari, M. Hijji, M. F. Allehyani, et al., Fractional-order dynamic modeling of renewable-dominant power systems using long-memory load and generation data, *Fractal Fract.*, **10** (2026), 183. https://doi.org/10.3390/fractalfract10030183
13. C. Feng, L. B. Huang, X. Q. He, Y. Wang, F. Dörfler, C. Q. Kang, Hybrid oscillation damping and inertia management for distributed energy resources, *IEEE Trans. Power Syst.*, **40** (2025), 5041–5056. https://doi.org/10.1109/TPWRS.2025.3562811
14. S. Q. Wang, Z. H. Zhao, Y. L. Li, The research progress on power system restoration and resilience analysis: key technologies and future development trends, *Adv. Resour. Res.*, **5** (2025), 2528–2558. https://doi.org/10.50908/arr.5.4_2528
15. S. Ćosić, I. Vokony, Advancements in AI-driven approaches for grid stability monitoring, In: *2025 10th International Youth Conference on Energy (IYCE)*, Budapest, Hungary, 2025, 1–7. https://doi.org/10.1109/IYCE66046.2025.11155020
16. A. Saxena, R. Shankar, E. F. El-Saadany, M. Kumar, O. Al Zaabi, K. Al Hosani, Intelligent load forecasting and renewable energy integration for enhanced grid reliability, *IEEE Trans. Ind. Appl.*, **60** (2024), 8403–8417. https://doi.org/10.1109/TIA.2024.3436471
17. A. Waheed, J. Y. Li, A hybrid machine learning approach for real-time reliability evaluation of power systems, *Phys. Scr.*, **100** (2025), 076016. https://doi.org/10.1088/1402-4896/ade644
18. S. K. A. Zaidi, K. S. A. Islam, M. T. Abbas, T. Abbas, Hybrid ML-based fault detection in renewable-integrated power grids, *Spectrum Eng. Sci.*, **3** (2025), 520–527.

19. P. Dineshkumar, Machine learning-based predictive stability assessment for renewable-rich power systems, *Natl. J. Intell. Power Syst. Technol.*, **2** (2026), 23–33.
20. K. Zeriouh, M. Amara, AI-driven frameworks for strategic risk management: a systematic review and model for organizational resilience and decision support, *J. Intell. Manag. Decision*, **4** (2025), 224–234. https://doi.org/10.56578/jimd040304
21. Y. Sanjalawe, S. Al-E' Mari, S. Fraihat, S. N. Makhadmeh, E. Alzubi, AI-powered smart grids in the 6G era: a comprehensive survey on security and intelligent energy systems, *IEEE Open J. Commun. Soc.*, **6** (2025), 7677–7719. https://doi.org/10.1109/OJCOMS.2025.3609144
22. M. Rouholamini, C. S. Wang, S. Magableh, X. S. Wang, Resiliency of electric power distribution networks: a review, *J. Infrastruct. Preserv. Resil.*, **6** (2025), 39. https://doi.org/10.1186/s43065-025-00154-y
23. O. Lordan, J. M. Sallan, P. Simo, Study of the topology and robustness of airline route networks from the complex network approach: a survey and research agenda, *J. Transp. Geogr.*, **37** (2014), 112–120. https://doi.org/10.1016/j.jtrangeo.2014.04.015
24. P. Linardatos, V. Papastefanopoulos, S. Kotsiantis, Explainable AI: a review of machine learning interpretability methods, *Entropy*, **23** (2021), 18. https://doi.org/10.3390/e23010018
25. Y. Tang, J. Kurths, W. Lin, E. Ott, L. Kocarev, Introduction to focus issue: When machine learning meets complex systems: networks, chaos, and nonlinear dynamics, *Chaos*, **30** (2020), 063151. https://doi.org/10.1063/5.0016505
26. M. Ayaz, T. Ali, M. Hijji, I. Baig, T. Alhmiedat, E. H. M. Aggoune, Predictive modeling of complex networks using deep learning and fractional dynamics, *AIMS Math.*, **10** (2025), 26717–26743. https://doi.org/10.3934/math.20251175
27. F. Li, Y. Z. Cai, L. Su, H. Shen, S. Y. Xu, $\mathcal{H}_\infty$ state estimation for two-time-scale Markov jump complex networks under analog fading channels: a hidden-Markov-model-based method, *IEEE Trans. Circuits Syst. I Regul. Pap.*, **71** (2024), 3833–3842. https://doi.org/10.1109/TCSI.2024.3372548
28. F. Li, Y. N. Wang, H. Shen, Dual event-triggered synchronization of two-time-scale jumping neural networks and its application in image encryption and decryption, *IEEE Trans. Netw. Sci. Eng.*, **12** (2025), 943–954. https://doi.org/10.1109/TNSE.2024.3521429
29. H. Shen, C. J. Peng, H. C. Yan, S. Y. Xu, Data-driven near optimization for fast sampling singularly perturbed systems, *IEEE Trans. Automat. Control*, **69** (2024), 4689–4694. https://doi.org/10.1109/TAC.2024.3352703
30. N. Zhao, D. Lun, H. Y. Zhang, X. D. Zhao, I. J. Rudas, Composite anti-disturbance control for networked systems with disturbances and actuator attacks via event-triggered output feedback, *IEEE Trans. Cybernet.*, **56** (2026), 393–403. https://doi.org/10.1109/TCYB.2025.3609819
31. T. Wu, J. H. Wang, Artificial intelligence for operation and control: the case of microgrids, *Electr. J.*, **34** (2021), 106890. https://doi.org/10.1016/j.tej.2020.106890
32. P. M. Peruman, K. Ayyar, Power quality disturbance identification using hybrid deep learning in renewable energy systems, *Sci. Rep.*, **15** (2025), 44592. https://doi.org/10.1038/s41598-025-28291-0

33. R. K. Priya, N. Karuppiah, H. Subhadra, P. K. Balachandran, Deep learning empowered cyber-physical intelligence system for resilient renewable aware IoT integrated smart grid systems, *Eng. Res. Express*, **8** (2026), 065211. https://doi.org/10.1088/2631-8695/ae4f5a

34. P. Sarajcev, A. Kunac, G. Petrovic, M. Despalatovic, Artificial intelligence techniques for power system transient stability assessment, *Energies*, **15** (2022), 507. https://doi.org/10.3390/en15020507

35. H. Xiang, X. L. Li, X. Liao, W. Cui, F. K. Liu, D. H. Li, Artificial intelligence in renewable energy systems: applications and security challenges, *Energies*, **18** (2025), 1931. https://doi.org/10.3390/en18081931

AIMS Press